

RESEARCH

Open Access



# Anti-inflammatory potential of *aspergillus unguis* SP51-EGY: TLR4-dependent effects & chemical diversity via Q-TOF LC-HRMS

Soad Nasr<sup>1,2†</sup>, Abdelhameed S. Dawood<sup>1†</sup>, Amal Mosad Ibrahim<sup>3</sup>, Mohamed S. Abdel-Aziz<sup>4</sup>, Walid Fayad<sup>5</sup>, Anwar Abdelnaser<sup>1\*</sup> and Faten K. Abd EL-Hady<sup>3</sup>

## Abstract

Inflammation serves as an intricate defense mechanism for tissue repair. However, overactivation of TLR4-mediated inflammation by lipopolysaccharide (LPS) can lead to detrimental outcomes such as sepsis, acute lung injury, and chronic inflammation, often associated with cancer and autoimmune diseases. This study delves into the anti-inflammatory properties of "*Aspergillus unguis* isolate SP51-EGY" on LPS-stimulated RAW 264.7 macrophages. Through real-time qPCR, we assessed the expression levels of pivotal inflammatory genes, including iNOS, COX-2, TNF- $\alpha$ , and IL-6. Remarkably, our fungal extracts significantly diminished NO production and showed noteworthy reductions in the mRNA expression levels of the aforementioned genes. Furthermore, while Nrf2 is typically associated with modulating inflammatory responses, our findings indicate that the anti-inflammatory effects of our extracts are not Nrf2-dependent. Moreover, the chemical diversity of the potent extract (B Sh F) was elucidated using Q-TOF LC-HRMS, identifying 54 compounds, some of which played vital roles in suppressing inflammation. Most notably, compounds like granisetron, fenofibrate, and umbelliprenin were found to downregulate TNF- $\alpha$ , IL-1 $\beta$ , and IL-6 through the NF- $\kappa$ B signaling pathway. In conclusion, "*Aspergillus unguis* isolate SP51-EGY", isolated from the Red Sea, Egypt, has been unveiled as a promising TLR4 inhibitor with significant anti-inflammatory potentials, presenting novel insights for their potential therapeutic use in inflammation.

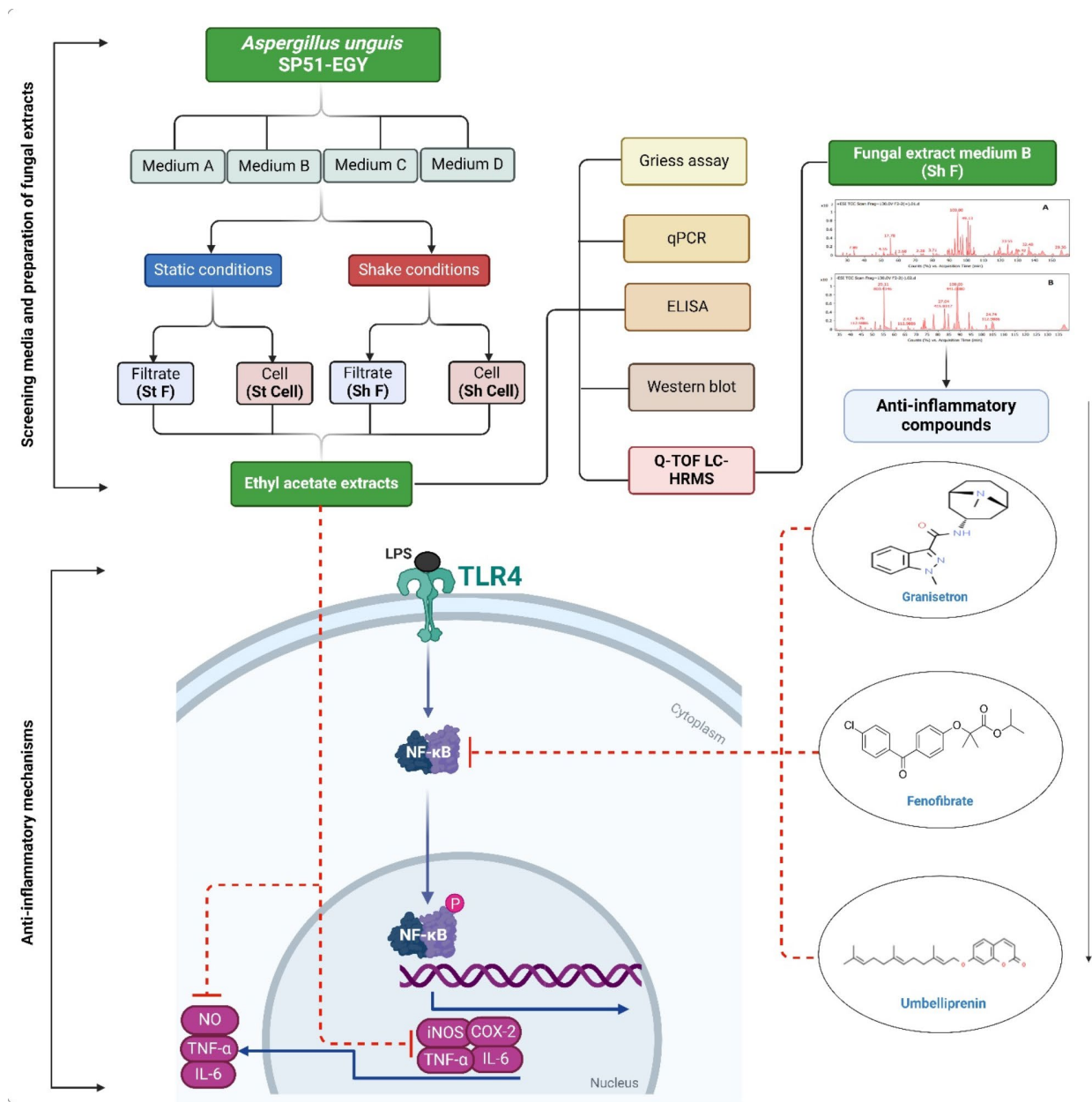
<sup>†</sup>Soad Nasr and Abdelhameed S. Dawood contributed equally to this work and share first authorship.

\*Correspondence:  
Anwar Abdelnaser  
anwar.abdelnaser@aucegypt.edu

Full list of author information is available at the end of the article



Graphical abstract



**Keywords** *Aspergillus unguis* SP51-EGY, TLR4, Anti-inflammatory, Macrophages, Q-TOF LC-HRMS

Introduction

After injury or infection, an innate immune response arises in the body, leading to inflammation. Inflammation is considered a complex defense machinery to repair tissues in the body [1]. The first line of defense to eradicate infections is macrophages. Toll-like receptors (TLRs) signaling pathways are activated by macrophages via lipopolysaccharide (LPS) with TLR4 ligates. This serves as an activating signal which leads to the

initiation of intracellular pathways [2]. The first inflammatory response involves the release of prostaglandins, histamine, and nitric oxide (NO) by inducible nitric oxide synthase (iNOS), which results in vasodilation, increased blood flow, and recruitment of leukocytes. Following activation of immune cells, pro-inflammatory cytokines like interleukin-6 (IL-6), interleukin-1 (IL-1), and tumor necrosis factor-alpha (TNF-α) escalate leukocyte permeability in the vascular regions by increasing leukocyte

adhesion to endothelial cells. Homeostasis is necessary during inflammation as prolonged inflammation could lead to serious health issues [2, 3]. In addition, the nuclear factor erythroid 2-related factor 2 (Nrf2) is the primary redox homeostasis regulator. Nrf2 plays a crucial role in protecting cells from inflammation and oxidative stress by regulating the expression of phase II detoxification enzymes and oxidative stress response proteins, such as heme oxygenase-1 (HO-1), and oxidative stress-induced growth inhibitor 1 (OSGIN1) [4, 5].

Natural products have been used since the beginning of time for healing applications. Currently, natural products are being used for the treatment of inflammatory diseases. Previously discovered herbal extracts have been shown to have key effects on TLR4 signaling pathways, a significant pathway for a pro-inflammatory response in the body [6]. In addition, natural extracts have been shown to employ their anti-inflammatory effects by regulating the expression of pro-inflammatory cytokines in LPS-induced inflammatory response [7].

Marine-associated fungi have an excellent provenance for secondary metabolites, many of which have diverse biological activities and highly complicated structures, making them hard to provide economically via chemical synthesis [8]. Furthermore, marine microorganisms can be cultured easily, which spreads high reproducibility and is a continual source of natural products [9]. The *Aspergillus* genus contains more than 300 species that live in a variety of habitats, of which the marine-derived species produce variable structures of secondary metabolites, like alkaloids, phenolics, terpenoids, and peptides with prominent biological effects such as cytotoxic, antimicrobial, and anti-inflammatory activities [10]. However, little is known about the chemical constituents and biological activities of “*Aspergillus unguis* isolate SP51-EGY” from the Red Sea, except that our previous work reported its antidiabetic effect [11]. Liquid chromatography-high-resolution mass spectrometry (LC-HRMS) is the dominant way to attain pure natural products for structure elucidation and evolution into therapeutic agents. In recent years, LC-HRMS use in natural product chemistry has grown in popularity, allowing for various analytical platforms for non-targeted, targeted, and suspect screening. LC-HRMS provides valuable structural input for detecting and exploring chemical substances identified from natural products [12].

This study aimed to find the highly effective anti-inflammatory fungal extract and to identify its secondary metabolites using LC-HRMS, which plays an essential role in determining accurate masses and is used for comprehensive analysis in both positive and negative ionization modes to identify chemical compositions. This study proved that LC-HRMS is an efficacious and powerful analytical appliance for characterizing most of the

identified compounds of “*Aspergillus unguis* isolate SP51-EGY” from Red Sea, Egypt.

## Materials and methods

### Materials

The RAW 264.7 cell line was purchased from the American Type Culture Collection (ATCC TIB-71; RRID: CVCL\_0493). LPS (*Escherichia coli* O111:B4) was purchased from Sigma-Aldrich (St. Louis, MO, USA). QIAzol Lysis Reagent and Nuclease-free water were obtained from Qiagen (Hilden, Germany). Dimethyl Sulfoxide (DMSO), Methanol, Chloroform, Isopropanol, and Ethanol were of HPLC grade and were all purchased from SERVA (Heidelberg, Germany). Cyclooxygenase-2 (COX-2) Polyclonal Antibody, Mouse TNF- $\alpha$ , and Mouse IL-6 ELISA Kits were purchased from Elabscience (Wuhan, China). Dulbecco's Modified Eagle Medium (DMEM), Phosphate Buffered Saline (PBS), Fetal Bovine Serum (FBS), Penicillin-Streptomycin (Pen/Strep), (3-(4,5-dimethylthiazol-2-yl)-2,5-diphenyltetrazolium bromide (MTT), Griess Reagent Kit, RevertAid First Strand cDNA Synthesis Kit, PowerUp™ SYBR™ Green Master Mix, mRNA primers (iNOS, COX-2, TNF- $\alpha$ , IL-6, COX-2 and GAPDH), Pierce™ BCA Protein Assay Kit, Pierce™ 20X TBS Tween™ 20 Buffer, Blocker™ BSA (10X) in PBS, GAPDH Polyclonal Antibody, Goat Anti-Rabbit IgG (H+L) Secondary Antibody, Horseradish Peroxidase (HRP)-conjugated, and Pierce™ ECL Western Blotting Substrate were all purchased from Thermo Fisher Scientific (Waltham, MA, USA). Cell Lysis Buffer (10X), Protease Inhibitor Cocktail (100X), and Prestained Protein Marker, Broad Range (11–190 kDa) were purchased from Cell Signaling (Danvers, MA, USA). Heme Oxygenase-1 (HO-1), Oxidative Stress-Induced Growth Inhibitor-1 (OSGIN1) mRNA primers were ordered from Synbio Technologies (Monmouth Junction, NJ, USA).

### Sponge materials and molecular identification of the fungal isolate

The Sponge (*Agelas* sp.) was gathered from the coast of Hurghada, Red Sea, Egypt (Shaab al-Ariq latitude, N 27° 25' 08.9", E 33° 51' 0.5). Sponge sample was used according to Aboutabl et al. [11]. The fungus was identified as “*Aspergillus unguis* isolate SP51-EGY”. The sequence has been deposited in GenBank with the name *Aspergillus unguis* isolate SP51-EGY and accession number KM203831.1 [11].

### Screening media and preparation of fungal extracts

For the fungus cultivation, four different broth media (A, B, C, and D) were used. The media were made up of the following components (g/L): Medium A (Sabouraud broth) contains dextrose (20 g/L) and peptone (10 g/L); Medium B (Nutrient broth) contains peptone (5 g/L),

beef extract (1 g/L), yeast extract (2 g/L), and sodium chloride (6 g/L); Medium C (Potato dextrose broth) contains dextrose (20 g/L) and potato-infusion (200 g/L); Medium D (Malt extract broth) contains yeast extract (3 g/L) and malt extract (17 g/L). Secondary metabolite ethyl acetate extracts from static and shake conditions were abbreviated as: **Sh F** (shake filtrate) extract, **Sh Cell** (shake mycelia) extract, **St F** (static filtrate) extract, and **St Cell** (static mycelia) extract.

#### Cell culture

RAW 264.7 cells were cultured in a 5% CO<sub>2</sub> humidified incubator at 37 °C in DMEM supplemented with 10% heat-inactivated FBS and 1% Pen-Strep (100 units/mL penicillin, and 100 µg/mL streptomycin).

#### Determination of NO production using Griess method

RAW 264.7 cells were cultured in a 96-well plate for 2 h at a seeding density of  $1 \times 10^6$  cells/mL. The cells were then stimulated with LPS (10 ng/mL) and co-treated with different fungal extracts at concentration of 10 µg/mL for 24 h. The NO production in the cell culture medium was determined using the Griess method through mixing 150 µL of the culture supernatant from each well with 130 µL of deionized water and 20 µL of Griess reagent and incubating for 30 min in the dark at room temperature as previously described [13]. The absorbance was measured at 548 nm using SPECTROstar® Nano microplate reader (BMG LABTECH, Germany). NO concentration in each sample was eventually calculated using a NaNO<sub>2</sub> standard curve.

#### Determination of cytotoxicity using MTT assay

To confirm that the anti-inflammatory effect of the fungal extracts was not a result of cytotoxicity, MTT colorimetric assay was performed. On the 96-well plate containing cultured RAW 264.7 macrophages from the Griess

experiment, MTT solution was added (1 mg/mL) for 2 h at 37°C. MTT solution was then discarded and a volume of 100 µL of DMSO was added in order to solubilize the formed formazan crystals. The absorbance was measured at 540 nm using SPECTROstar® Nano microplate reader. Cell viability percentage was then determined relative to the control group.

#### Isolation of total RNA

RAW 264.7 cells were seeded at a density of  $1 \times 10^6$  cells/mL in 6-well plates and incubated overnight. The cells were then stimulated with LPS (10 ng/mL) and co-treated with different fungal extracts at concentration of 10 µg/mL for 6 h. Total RNA was extracted from the cells using QiAzol lysis reagent. An amount of 1 µg of RNA from each sample was used to synthesize the cDNA using RevertAid First Strand cDNA Synthesis Kit according to manufacturer's protocol. cDNA was stored in -20 °C for further use in mRNA expression analysis.

#### Determination of inflammatory mRNA expression levels using quantitative real-time polymerase chain reaction (qPCR)

The qPCR was used for the determination of inflammatory mRNA expression levels. The cDNA was mixed with forward and reverse primers (Table 1), maxima SYBR green mix, and nuclease free water. The inflammatory genes selected for this experiment are: iNOS, COX-2, TNF-α, and IL-6. All mRNA expression levels were normalized to endogenous control (GAPDH) and the  $2^{-\Delta\Delta CT}$  method was used to evaluate the relative fold mRNA expression levels. The qPCR analysis was performed using ABI Prism 7500 system (Applied Biosystems) under the following conditions: initial holding stage at 95 °C for 10 min, followed by 40 PCR cycles of denaturation at 95 °C for 15 s and annealing/extension at 60 °C for 1 min. Primer design generation was done using NCBI Primer-Blast tool (Table 1).

#### Determination of mRNA expression levels of Nrf2-driven ARE genes HO-1 and OSGIN1 in LPS-stimulated RAW 264.7 macrophages.

The qPCR primers for Nrf2-driven ARE Genes HO-1 and OSGIN1 were used to determine whether the anti-inflammatory activity of the fungal extracts was associated with Nrf2 signaling pathway. The qPCR reactions were subjected to the same thermocycling conditions as the previous experiment. All mRNA expression levels were normalized to endogenous control (GAPDH) and the  $2^{-\Delta\Delta CT}$  method was used to evaluate the relative fold mRNA expression levels.

**Table 1** mRNA sequences used for qPCR

Target mRNA	Primer sequence (5'-3')	Tm
iNOS	Forward: GGAACCTACCAGCTCACTCTGG	63
	Reverse: TGCTGAAACATTTCTGTGCTGT	60
COX-2	Forward: CTCACGAAGGAACTCAGCAC	58
	Reverse: GGATTGGAACAGCAAGGATTTG	58
TNF-α	Forward: GAACTCCAGCGGTGCCAT	63
	Reverse: TGAGAGGGAGGCCATTTGGG	63
IL-6	Forward: GATGCTACCAAAGTGGATATAATCAG	55
	Reverse: CTCTGAAGGACTCTGGCTTTG	58
HO-1	Forward: CACAGATGGCGTCACTTCGTC	60
	Reverse: GTGAGGACCCACTGGAGGAG	62
OSGIN1	Forward: CGGTGACATCGCCACTAC	62
	Reverse: GCTCGGACTTAGCCCACTC	62
GAPDH	Forward: CTTTGTCAAGCTCATTTCCTGG	57
	Reverse: TCTTGCTCAGTGCTCTTGC	58

### Quantification of the pro-inflammatory cytokine protein levels using enzyme-linked immunosorbent assay (ELISA)

Protein expression levels of the pro-inflammatory cytokines, TNF- $\alpha$  and IL-6, were quantified by pre-coated ELISA plates (Elabscience<sup>®</sup>) according to the manufacturer's protocol. RAW 264.7 cells were seeded in 6-well plates ( $1 \times 10^6$  cells/mL) and incubated overnight. The cells were then stimulated with LPS (10 ng/mL) and co-treated with different fungal extracts at concentration of 10  $\mu$ g/mL for 24 h. After incubation, the supernatants were collected, centrifuged at  $1000 \times g$  for 20 min at 4  $^{\circ}$ C and then transferred to new microcentrifuge tubes to analyze the level of TNF- $\alpha$  and IL-6 proteins secreted into the cell culture medium. The supernatant was diluted in a ratio of 1:100 for TNF- $\alpha$  and 1:20 for IL-6 in buffered sample diluent. The absorbance was measured at 450 nm using SPECTROstar<sup>®</sup> Nano microplate reader.

### Western blotting

Protein expression level of COX-2 was determined using Western blotting. RAW 264.7 cells were seeded in 6-well plates ( $1 \times 10^6$  cells/mL) and incubated overnight. The cells were then stimulated with LPS (10 ng/mL) and co-treated with different fungal extracts at concentration of 10  $\mu$ g/mL for 24 h. Total proteins were extracted from the cells using cell lysis buffer containing a protease inhibitor cocktail, and the protein concentration was measured using Pierce<sup>™</sup> BCA Protein Assay Kit. Western blotting was performed using a standard protocol. Briefly, proteins (10  $\mu$ g) were separated by 10% SDS-PAGE and transferred to a PVDF membrane. After blocking with 5% non-fat dry milk in TBST for 1 h at room temperature, the membrane was incubated with primary antibodies; anti-COX-2 antibody (1:1000 dilution), and anti-GAPDH antibody (1:2500 dilution) overnight at 4  $^{\circ}$ C. After washing three times with TBST, the membrane was incubated with HRP-conjugated secondary antibody (1:15000 dilution) for 1 h at room temperature. Protein bands were visualized with Pierce<sup>™</sup> ECL Western Blotting Substrate using ChemiDoc MP Imaging System (Bio-Rad Laboratories, CA, USA).

### Q-TOF LC-HRMS spectroscopy analysis

For chromatographic separation, a 6530 Q-TOF LC/MS (Agilent Technologies) equipped with an autosampler (G7129A), a Quat. Pump (G7104C), and a Column Comp (G7116A) were used at the Faculty of Pharmacy, Fayoum University. The injection volume was set at 5  $\mu$ L. The analytes were separated on an Agilent Technologies Zorbax RP-18 column (dimensions: 150 mm  $\times$  3 mm,  $d_p$ =2.7  $\mu$ m) at a flow rate of 0.3 mL/min. ESI was used to obtain mass spectra in (+) and (-) ionization modes with a capillary voltage of 4500 V. The mass spectra were recorded in the 50–3000  $m/z$  range. The gas temperature and drying gas

flow were 200  $^{\circ}$ C and 8 L/min, respectively. The skimmer and fragmentator voltages were set at 65 and 130 V, respectively, and collision energy was 10 V. The nebulization pressure was 58 psig. Elution was with Solvent A (Water 0.1% formic acid) and Solvent B (Acetonitrile 0.1% formic acid), the flow rate was 0.3 mL/min. Gradient elution started with 2% B, reaches 10% B at 15 min and 20% B at 35 min, 50% B at 60 min, 70% B at 80 min and then 100% B at 100 min.

### Statistical analysis

Statistical significance between groups was determined using one-way analysis of variance (ANOVA) followed by Student–Newman–Keuls post hoc test, where  $P$ -value < 0.05 was considered statistically significant. The data from three independent experiments are presented as the mean  $\pm$  standard error of the mean (SE). Comparative analysis between experimental groups was performed using SigmaPlot (Version 14.0; Systat Software, Chicago, IL, USA).

## Results and discussion

### Determination of NO production in LPS-stimulated RAW

#### 264.7 macrophages

Macrophages play a key role in the innate immune response [14, 15]. LPS, a major component in the cell wall of gram-negative bacteria can induce the production of inflammatory mediators, and is frequently used to evaluate the anti-inflammatory effects of drugs [16]. The production of inflammatory mediators including NO is increased in LPS-stimulated macrophages. NO is a bioactive signaling molecule which has a key role in modulating the inflammatory response [17]. Therefore, the anti-inflammatory effect of the fungal extracts was evaluated using LPS-stimulated RAW 264.7 macrophages. The NO production in the cell culture medium was determined using the Griess method and according to the measured  $\text{NaNO}_2$  standard curve. It was shown that NO production was significantly increased in the cell culture medium of LPS-stimulated macrophages (19.8  $\mu$ M) compared to the control (11.2  $\mu$ M).

As for the extracts in medium (A–D), NO production was significantly reduced in all samples in medium A and C in comparison to LPS-stimulated cells. As for medium B, only Sh F and St Cell extracts significantly reduced NO production, resulting in levels of 12.9  $\mu$ M and 14.4  $\mu$ M, respectively, in comparison to LPS-stimulated cells, and for medium D, Sh F and Sh Cell extracts significantly reduced NO production, resulting in levels of 7.2  $\mu$ M and 6.8  $\mu$ M, respectively, in comparison to LPS-stimulated cells (Fig. 1). These results validate that some of the fungal extracts have significant effect on reducing NO production in LPS-stimulated RAW 264.7 cells and highlight

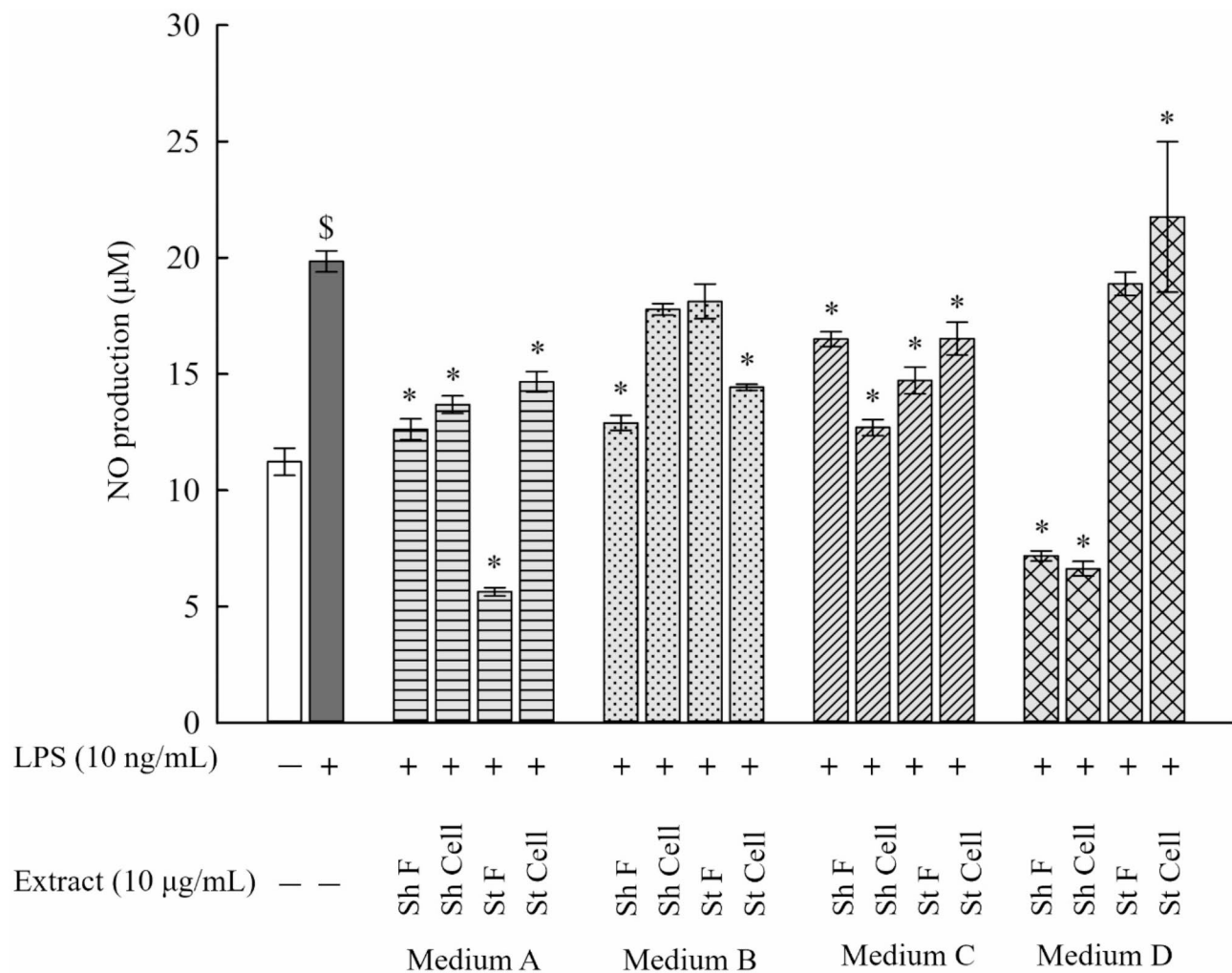


**Fig. 1** Measurement of NO production of extracts found in medium (A-D) on RAW 264.7 macrophages. After treatment of LPS-stimulated RAW 264.7 macrophages ( $1 \times 10^6$  cells/mL) with 10 µg/mL of extracts in medium (A-D) and cultured overnight. NO production in the cell culture medium was measured using the Griess method. LPS-stimulated cells only showed high significance in comparison to control. All extracts in medium A and medium C showed a significant decrease in NO production in comparison to LPS-stimulated cells. However, Sh Cell and St F extracts in medium B and St F and St Cell in medium D did not show any significant decrease in comparison to LPS-stimulated cells. Results are presented as the mean  $\pm$  SE ( $n=3$ ). Statistical significance was calculated by one-way ANOVA followed by Student–Newman–Keuls post-hoc test. \$  $P < 0.05$  vs. control cells. \*  $P < 0.05$  vs. LPS-stimulated cells

the potential anti-inflammatory effect on RAW 264.7 cells [18].

To ensure that the observed NO reduction was not due to a reduction in cell viability, MTT assay was used to measure the cytotoxicity of RAW 264.7 macrophages after treatment with the extracts (medium A-D). Our results showed that no cytotoxicity was observed at the tested concentrations on the cultured cells. As a result, the reduction in NO production observed in the LPS-stimulated cells after treatment with the extracts was not due to cytotoxicity. The anti-inflammatory effect of these extracts was further experimented on to assess their anti-inflammatory effect using the same concentration (10 µg/mL) of NO production (Fig. 2).

#### Determination of mRNA expression levels of the pro-inflammatory markers iNOS, COX-2, TNF $\alpha$ , and IL-6 in LPS-stimulated RAW 264.7 macrophages

During inflammation, the immune system triggers the production of pro-inflammatory cytokines (TNF- $\alpha$ , IL-6), as well as enzymes (iNOS, COX-2) [19]. Current research is emphasizing the exploration of bioactive compounds with the capacity to suppress the production of these inflammatory mediators. Natural products are gaining attention as potent and safe anti-inflammatory agents, owing to their capability to modulate gene expression of diverse inflammatory mediators, thus offering promising avenues for therapeutic intervention [20]. Hence, to investigate the anti-inflammatory activities of the fungal extracts, the mRNA expression level of iNOS, COX-2, TNF- $\alpha$ , and IL-6 was determined using qPCR

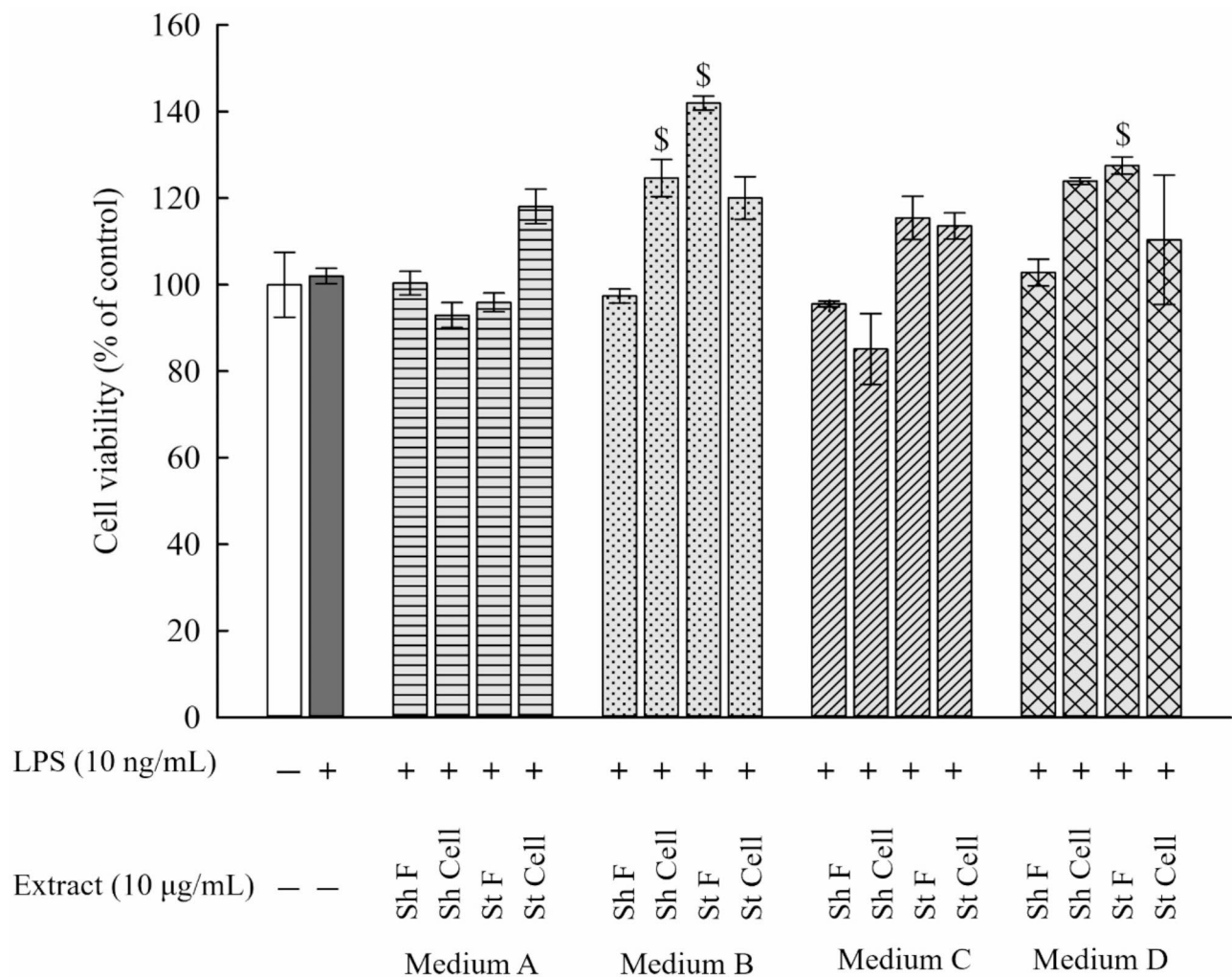


**Fig. 2** Measurement of cytotoxicity on RAW 264.7 macrophages using MTT assay. After treatment of LPS-stimulated cells with 10 µg/mL of extracts found in medium (A-D) and cultured overnight, cell viability was determined using MTT assay. All extracts in medium (A-D) did not show any cytotoxicity on RAW 264.7 cells. Results are presented as the mean  $\pm$  SE ( $n=3$ ). Statistical significance was calculated by one-way ANOVA followed by Student–Newman–Keuls post-hoc test. \$  $P < 0.05$  vs. control cells. \*  $P < 0.05$  vs. LPS-stimulated cells

(Fig. 3). Overall, eight samples from the different extraction media, with the highest anti-inflammatory action as evidenced by Griess assay, were selected for further anti-inflammatory studies. The results from qPCR further confirmed our previous results obtained from the Griess analysis. For LPS-stimulated macrophages, significant upregulation was observed for iNOS, COX-2, TNF- $\alpha$ , and IL-6 mRNA levels compared to the control. After treatment with the fungal extracts, the mRNA expression levels were significantly reduced. For the iNOS mRNA expression levels, significant reduction was observed for Sh F and St Cell in medium B, and Sh Cell in medium C (Fig. 3A). As for COX-2 mRNA expression levels, all samples in medium (A-D) showed a highly significant reduction in COX-2 expression in comparison to LPS-stimulated macrophages (Fig. 3B). Furthermore, the following samples showed significant reduction in TNF- $\alpha$

mRNA expression levels: Sh F in medium A, Sh F and St Cell in medium B, Sh Cell in medium C, and Sh F in medium D. However, St F (medium A), St F (medium C) and Sh Cell (medium D) did not show any significant reduction in TNF- $\alpha$  mRNA expression levels (Fig. 3C). Finally, for IL-6 mRNA expression levels, all 8 samples in all extraction medium (medium A-D) showed a highly significant reduction in IL-6 mRNA expression levels in comparison to LPS-stimulated macrophages (Fig. 3D). Our findings are in agreement with the results reported by Anh et al. indicating that nitrogen-containing secondary metabolites from *Aspergillus unguis* showed anti-inflammatory activity by suppressing the production of NO and the expression of iNOS and IL-6 in LPS-stimulated RAW 264.7 macrophages [21]. In a previous study conducted by Cao et al., it has also been demonstrated that sterols isolated from *Aspergillus unguis* inhibited the

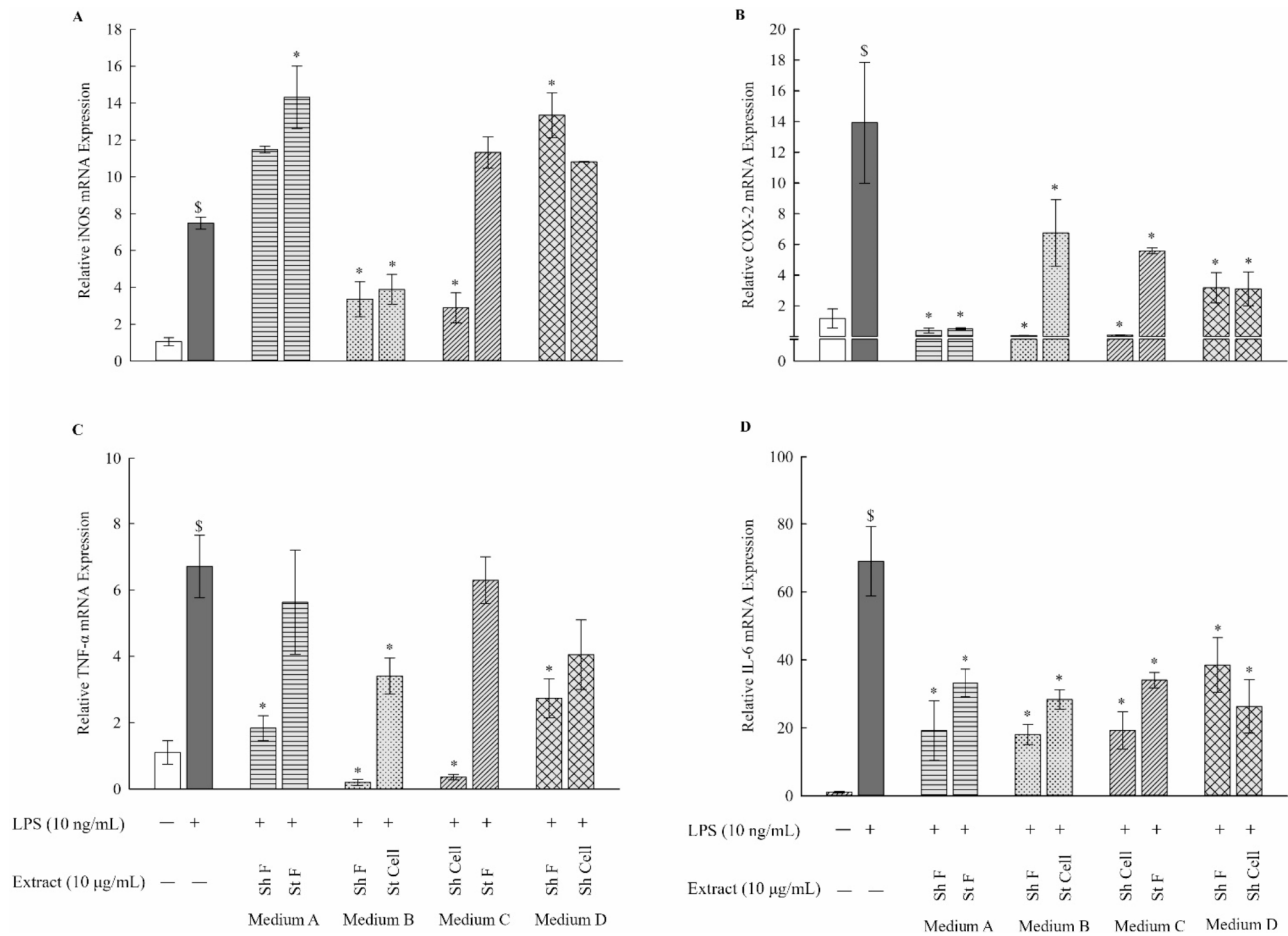


**Fig. 3** Expression levels of iNOS, COX-2, TNF- $\alpha$ , and IL-6 mRNA in LPS-stimulated RAW 264.7 macrophages. Fungal extracts in medium A-D (10  $\mu$ g/mL) were used for treatment of LPS-stimulated RAW 264.7 macrophages (LPS concentration: 10 ng/mL). The mRNA levels of iNOS, COX-2, TNF- $\alpha$  and IL-6 were measured using qPCR by the comparative method ( $2^{-\Delta\Delta CT}$ ). Results are presented as the mean  $\pm$  SE ( $n=3$ ). Statistical significance was calculated by one-way ANOVA followed by Student–Newman–Keuls post-hoc test. \$  $P < 0.05$  vs. control cells. \*  $P < 0.05$  vs. LPS-stimulated cells

production of inflammatory mediators, including NO and IL-6, along with downregulation of iNOS and IL-6 expressions in LPS-stimulated RAW 264.7 macrophages [22].

**Determination of mRNA expression levels of Nrf2-driven ARE genes HO-1 and OSGIN1 in LPS-stimulated RAW 264.7 macrophages**

The Nrf2-antioxidant response element (ARE) signaling pathway, which is recognized as a key regulatory system maintaining the intracellular redox homeostasis, also has a role in reducing inflammation [4]. The Nrf2-ARE activity can be attributed to modulating the expression of antioxidant and detoxifying enzymes, such as HO-1 and OSGIN1 [23, 24]. Additionally, recent studies demonstrated a correlation between the expression of inflammatory mediators, the NF- $\kappa$ B pathway, macrophage metabolism, and the Nrf2/ARE system [25]. To examine whether the inhibitory effect of the selected fungal extracts on LPS-mediated inflammation in RAW

264.7 macrophages was related to activation of the Nrf2-driven genes, the mRNA expression levels of HO-1 and OSGIN1 was analyzed by qPCR. Our data showed no significant upregulation in HO-1 and OSGIN1 mRNA expression between control, LPS-stimulated cells, and treated groups in mediums A-D. This is an indication that both HO-1 and OSGIN1 are not affected by any of the treatments (Fig. 4). These results propose that the anti-inflammatory effects of the fungal extracts are Nrf2-independent.

**Determination of protein levels of the pro-inflammatory cytokines TNF $\alpha$  and IL-6 in LPSstimulated RAW 264.7 macrophages**

Cytokines are key signaling proteins, which are produced to regulate the interactions between different cell types involved in the immune response [26]. Cytokines are mainly produced by phagocytic cells and natural killer (NK) cells during innate immune responses, while they are mostly secreted by lymphocytes and

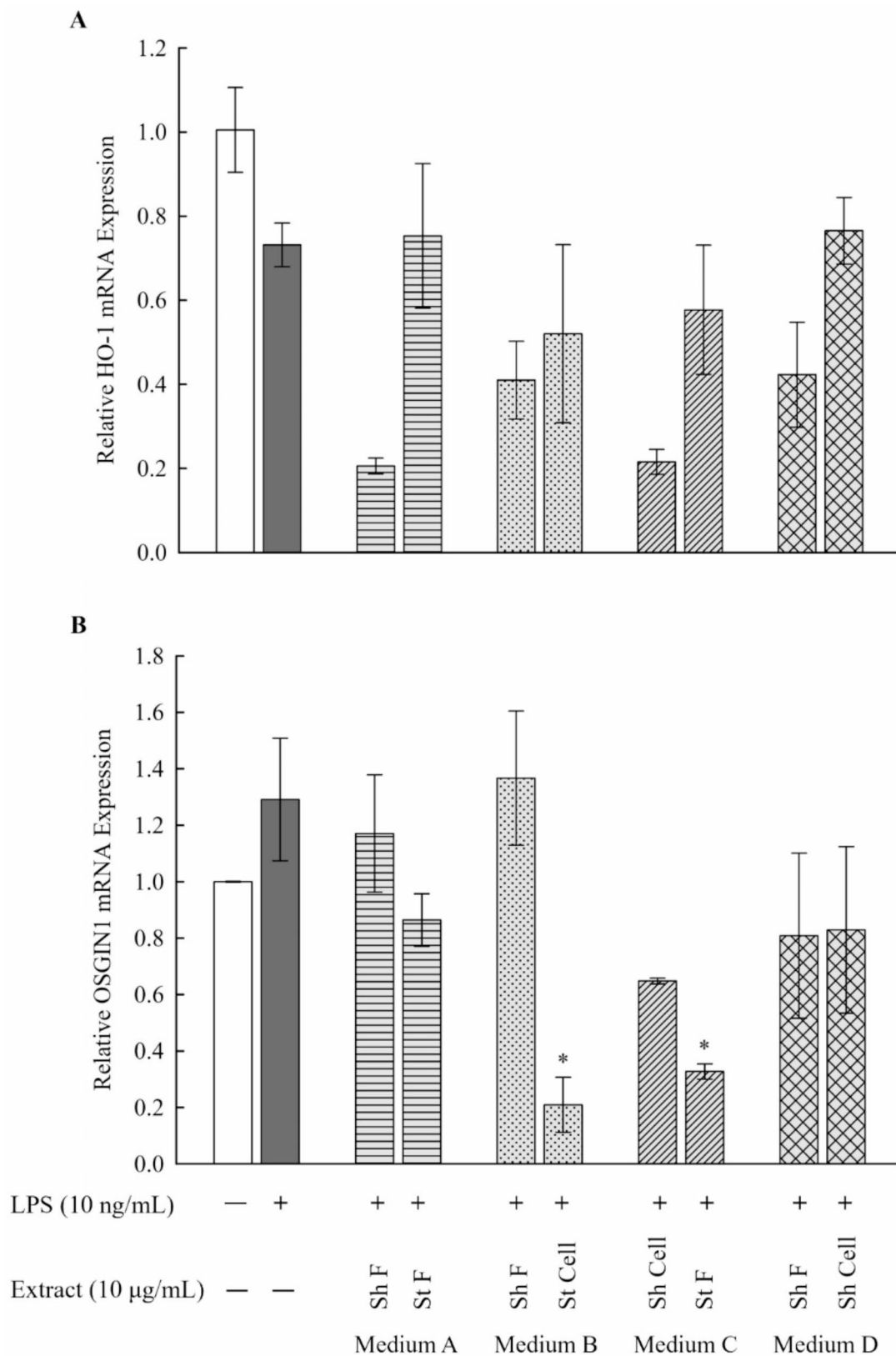


**Fig. 4** Expression levels of Nrf2-driven ARE genes, HO-1 (A) and OSGIN1 (B) mRNA in LPS-stimulated RAW 264.7 macrophages. Fungal extracts in medium A-D (10 µg/mL) were used for treatment of LPS-stimulated RAW 264.7 macrophages (LPS concentration: 10 ng/mL). The mRNA levels of HO-1 and OSGIN1 was measured using qPCR by the comparative method ( $2^{-\Delta\Delta CT}$ ). Results are presented as the mean  $\pm$  SE ( $n=3$ ). Statistical significance was calculated by one-way ANOVA followed by Student–Newman–Keuls post-hoc test. \$  $P < 0.05$  vs. control cells. \*  $P < 0.05$  vs. LPS-stimulated cells

antigen-presenting cells (APCs) during adaptive immune responses. Therefore, cytokines coordinate the cross-talk between the innate and adaptive immune systems. Among these, TNF- $\alpha$  and IL-6 are the major pro-inflammatory cytokines involved in the inflammatory response [27, 28]. In the present study, the protein expression levels of the pro-inflammatory cytokines TNF- $\alpha$  and IL-6, were assessed by ELISA. This was to confirm that the anti-inflammatory responses observed on the mRNA level carried through to the protein level. A concentration of 10 ng/mL of LPS significantly increased the pro-inflammatory response of RAW 264.7 macrophages as indicated by the elevated protein levels of the assessed cytokines (Fig. 5). However, at concentration of 10  $\mu$ g/mL of the selected fungal extracts (Sh F and St Cell in medium B and Sh Cell in medium C), significant reduction was observed in protein levels of the pro-inflammatory cytokines TNF $\alpha$  and IL-6 in LPSstimulated RAW 264.7 macrophages.

#### Determination of protein expression of COX-2 using western blotting

The iNOS induction in relation to COX-2 has been formerly reported in previous studies. In this context, it was shown that selective COX-2 inhibitors reduce COX-2-mediated generation of prostacyclin (PGI<sub>2</sub>). Moreover, PGI<sub>2</sub> was demonstrated to induce iNOS expression, resulting in the production of NO. Thus, it is likely that the fungal extracts might have reduced NO production via a selective inhibition of COX-2 [29]. A concentration of 10 ng/mL of LPS significantly increased the pro-inflammatory response of RAW 264.7 macrophages as indicated by the elevated protein levels of COX-2 (Fig. 6). However, at concentration of 10  $\mu$ g/mL of the selected fungal extracts (Sh F and St Cell in medium B and Sh Cell in medium C), significant reduction was observed in COX-2 protein levels in LPSstimulated RAW 264.7 macrophages.

#### Q-TOF LC-HRMS spectroscopy analysis

LC-MS coupled with QTOF is a cutting-edge analytical technique for identifying unknown bioactive compounds in natural product extracts. The key to obtaining pure natural products for structure elucidation and development into therapeutic agents is liquid chromatography-high-resolution mass spectrometry (LC-HRMS).

Based on the results of medium B extract (Sh F) represented by its significant anti-inflammatory effects, prompted us to investigate its chemical composition with Q-TOF LC-HRMS spectroscopy analysis. In our study, the chemical composition of a highly bioactive extract (Sh F) from medium B was elucidated using Q-TOF LC-HRMS analysis. All compounds were identified depending on their  $m/z$  value from MS spectra in both positive

and negative ionization modes ( $[M+H]^+/[M-H]^-$ , Fig. 7), using an Agilent LC/MS Mass Hunter Qualitative Software for preliminary identification, then confirmed from many other libraries databases (Figs. 8 and 9). In positive and negative ionization modes, Q-TOF LC-HRMS identified a total of 33 and 21 compounds, respectively (Table 2A, 2B).

#### Q-TOF LC-HRMS analysis [positive ionization mode]

According to our findings, the positive ionization mode was primarily characterized by the identified ions of peptides, fatty acids, amides, triglycerides, and others.

#### Peptides

The application of Q-TOF-MS/MS enabled the discovery of seven potentially bioactive peptides, including two isoleucyl-containing peptides, two phenylalanyl-containing peptides, two Histidiny-Cysteine isomers, and the polypeptide "Angiotensin IV." Their retention times (RT) were at 23.528, 27.265, 31.723, 33.901, 100.8, 101.92 and 53.456 min, respectively, and with molecular weights: 202.1323, 228.1483, 262.1327, 262.1329, 258.0784, 258.0785 and 774.4077  $m/z$ , respectively. The Q-TOF-MS/MS product ions of these peptides are given in (Table 2A).

#### Structural fragmentation study of peptides

For isoleucyl-alanine and L-isoleucyl-L-proline; the complementary ions produced by the cleavage of the amino-alkyl group's carbonyl C-C bond result in the characteristic fragment ion protonated "2-methylbutan-1-amine" with 86  $m/z$  ( $C_5H_{12}N$ ), Fig. 8).

Angiotensin IV has the molecular formula  $C_{40}H_{54}N_8O_8$ . The positive and negative ion modes of its precursor  $[M+H]^+$  and  $[M-H]^-$  ions have  $m/z$  775.4149 and 773.4022, respectively, with (RT) 53.456 and 53.428 min (Table 2A, 2B). The protonated and deprotonated angiotensin IV characteristic fragment ions were observed and identified in Fig. (9 A, 9B) (10 A, 10B).

The MS/MS spectrum in positive ionization mode shows three distinct pathways for fragmentation.

- **Pathway 1:** producing the characteristic product ion at the  $m/z$  399.2646  $[M+H-C_{20}H_{30}N_3O_4]^+$ .
- **Pathway 2:** showing fragments ions at  $m/z$  265.1774  $[M+H-C_{26}H_{35}N_6O_5]^+$ ,  $m/z$  72.0826  $[m/z$  265.1774( $C_{14}H_{19}N_2O_3$ ) -  $C_{10}H_{10}NO_3]^+$ .
- **Pathway 3:** showing fragments ions at  $m/z$  698.3222  $[M+H-C_6H_5]^+$  and at 551.2648  $[698.3222(C_{34}H_{49}N_8O_8)-C_4H_9-C_6H_5O]^+$ .

The data from the MS<sup>3</sup> spectrum of Angiotensin IV could further confirm this conclusion (Figs. 10A and 9A, Table 2A). On the other hand, Angiotensin IV

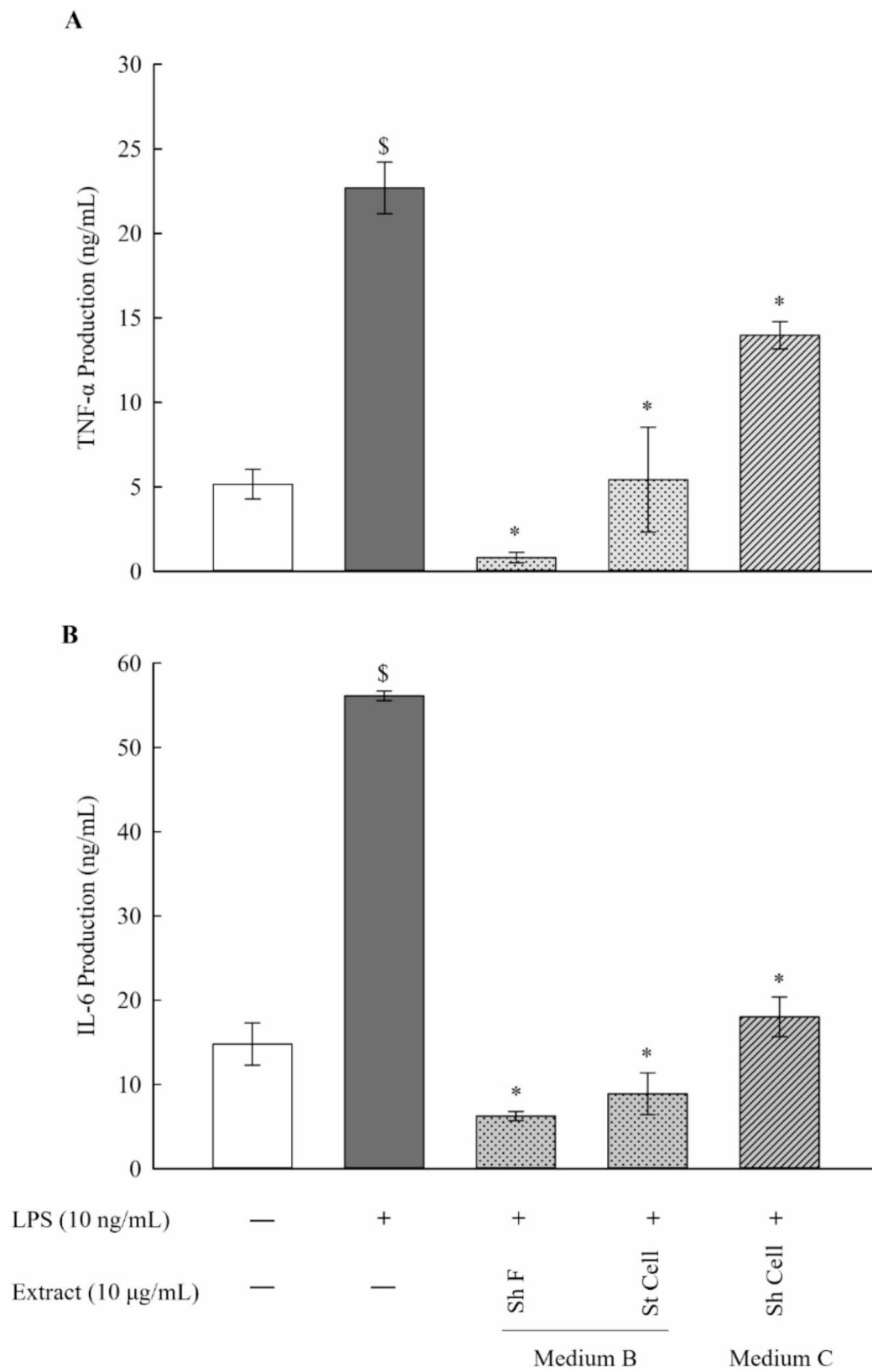


**Fig. 5** Determination of protein levels of the pro-inflammatory cytokines TNF- $\alpha$  and IL-6 in the cell culture medium of the LPS-stimulated RAW 264.7 macrophages using ELISA. The selected fungal extracts (Sh F and St Cell in medium B and Sh Cell in medium C) showed a significant reduction of the LPS-stimulated upregulation of the pro-inflammatory cytokines TNF- $\alpha$  (**A**) and IL-6 (**B**). Results are presented as the mean  $\pm$  SE ( $n=3$ ). Statistical significance was calculated by one-way ANOVA followed by Student–Newman–Keuls post-hoc test. \$  $P < 0.05$  vs. control cells. \*  $P < 0.05$  vs. LPS-stimulated cells

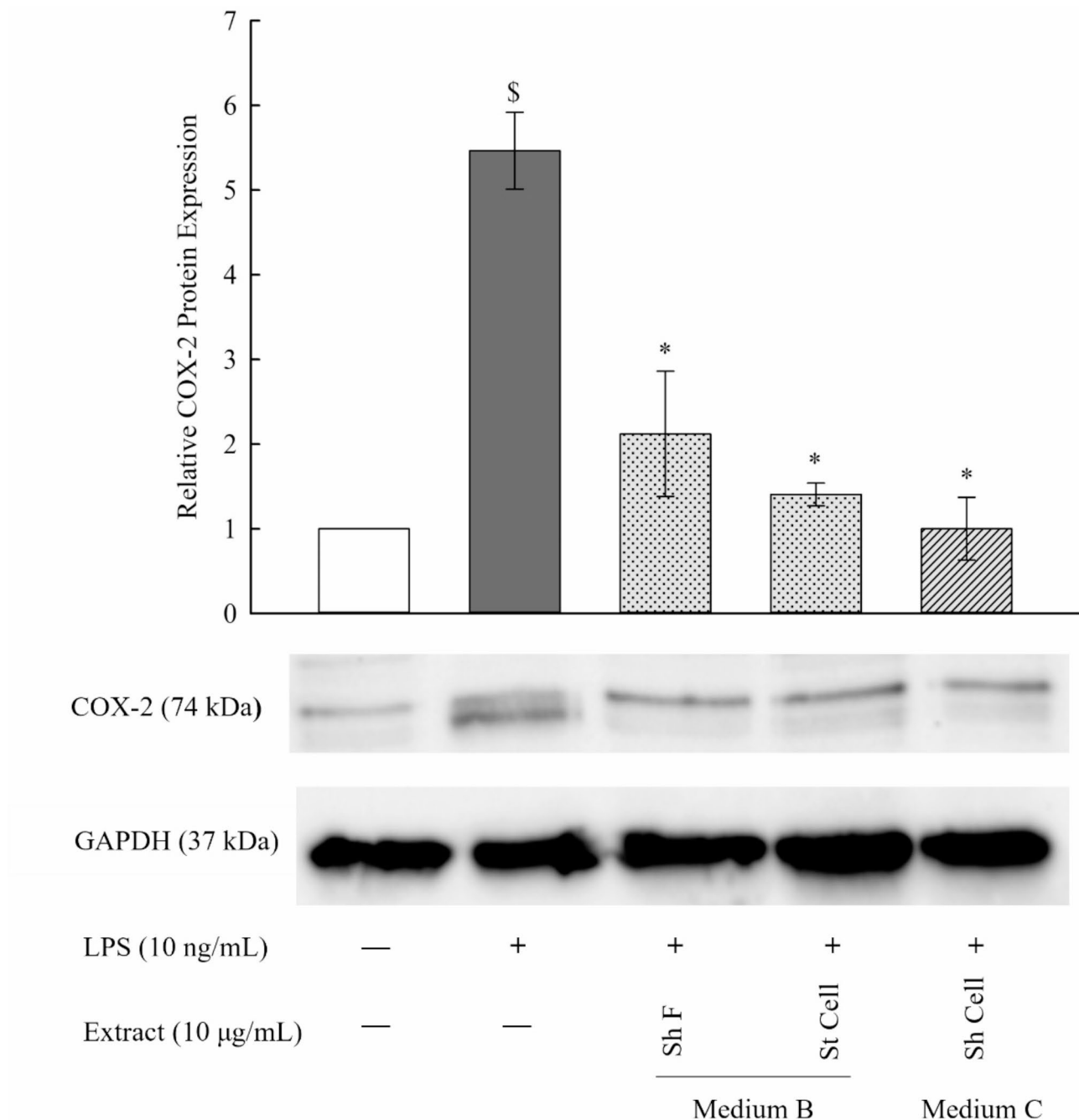


**Fig. 6** Western immunoblots and derived graphical illustration of the protein expression level for COX-2 in selected fungal extracts (Sh F and St Cell in medium B and Sh Cell in medium C). Results are presented as the mean ± SE (n=2). Statistical significance was calculated by one-way ANOVA followed by Student–Newman–Keuls post-hoc test. \$ P < 0.05 vs. control cells. \* P < 0.05 vs. LPS-stimulated cells

fragmentation in the negative ionization mode is followed by two pathways (Fig. 9B). Due to the loss of  $[M-H-C_{27}H_{35}N_6O_6-CH_3]^-$ , its characteristic minor fragment ion was observed at 221.0835 *m/z* in the first fragmentation pathway. Second fragmentation pathway: further fragmentation of precursor ion resulted in daughter ions at 432.2448 *m/z* due to loss of  $[M-H-C_6H_5O-C_3H_7-C_{10}H_{10}NO_3-H_2N]^-$  and 112.9869 *m/z*

due the loss of  $[(C_{16}H_{26}N_5O_2)]^-$  from the fragment 432.2448  $[(C_{21}H_{34}N_6O_4)]^-$  (Figs. 10B and 9B, Table 2B). The dissociation pattern of protonated Angiotensin IV  $[M+H]^+$  molecule consists essentially of five peaks in positive mode and three peaks in deprotonated Angiotensin IV  $[M-H]^-$  molecule in Negative mode. (Figure 9A and B). Protonated Angiotensin IV molecules produce

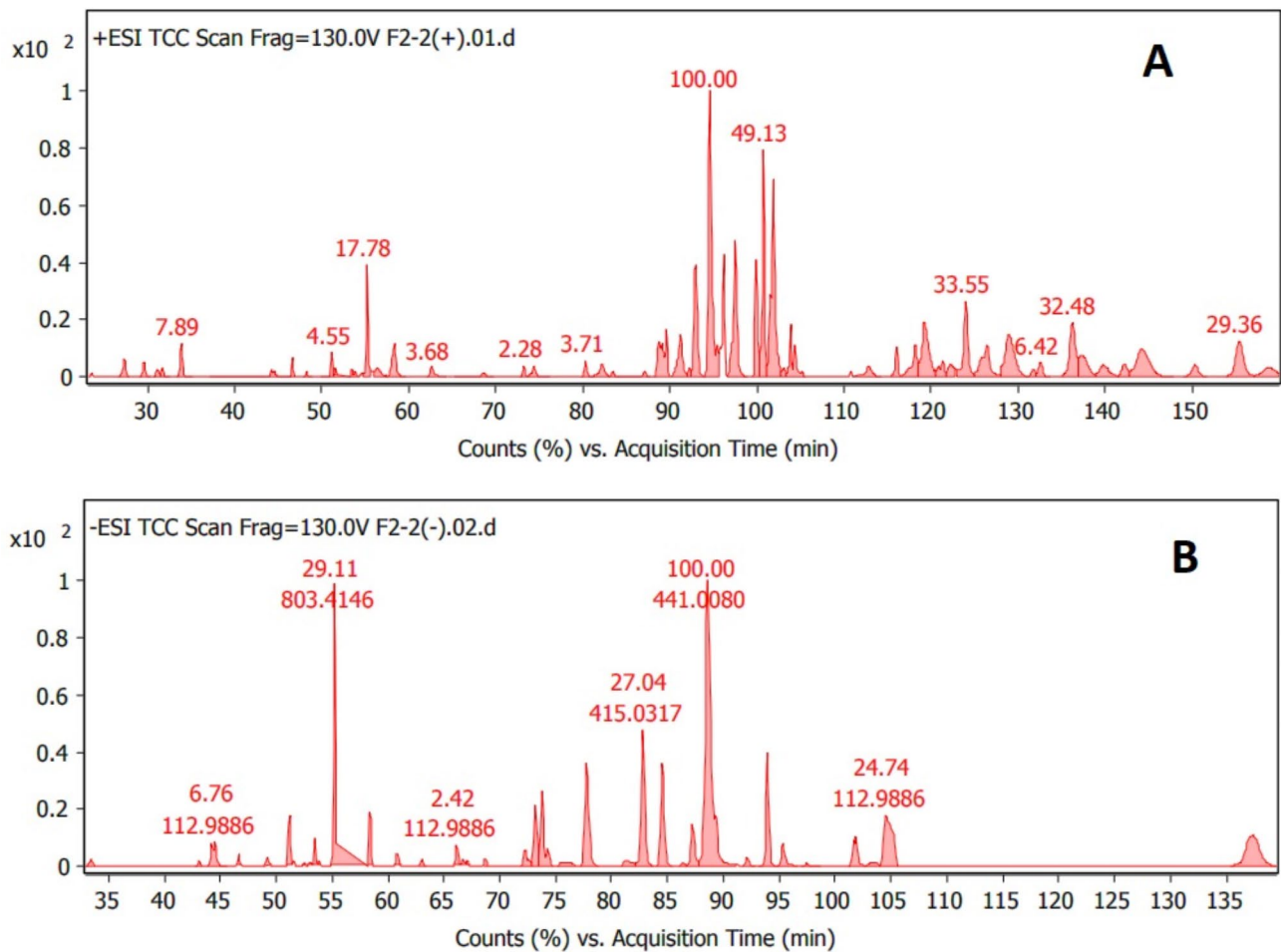


**Fig. 7** Total compound chromatogram (TCC) of Q-TOF LC-HRMS analysis of (B Sh F extract) for the fungus “*A. unguis* isolate SP51-EGY”; A=in positive, B=in negative ionization mode

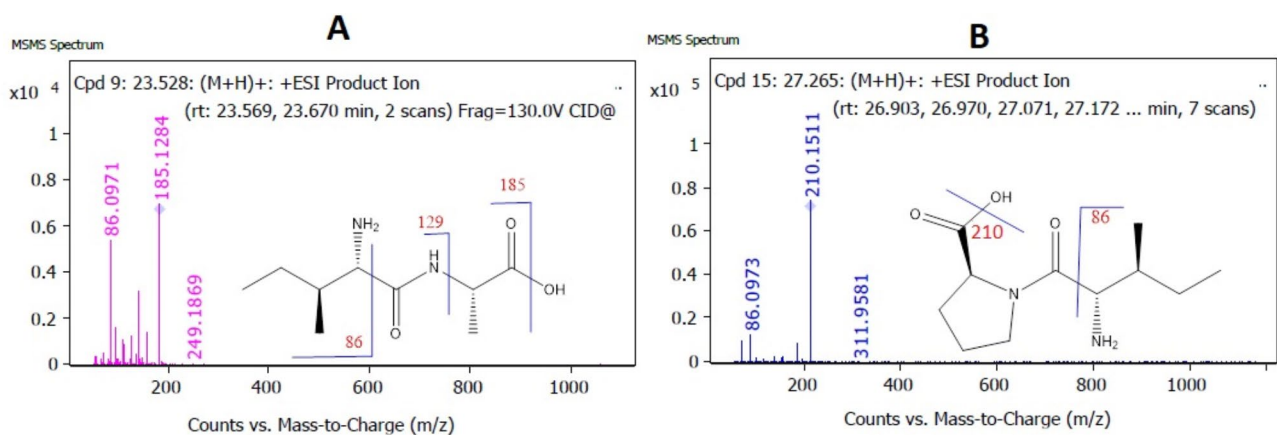


**Fig. 8** LC-Q-TOF mass spectrum ( $\text{ESI}^+$ ) of peptides and their proposed fragmentation patterns in positive-ion mode. **A**= Isoleucyl-Alanine,  $[\text{M} + \text{H}]^+$  with  $m/z$ 202) shows product ions with  $m/z$ 185 by the loss of  $\text{H}_2\text{O}$ , which further dissociated to produce a fragment ion at  $m/z$ 129 and 86 due to elimination of  $(\text{C}_3\text{H}_5\text{O}_2)$ ,  $(\text{C}_4\text{H}_6\text{NO}_3)$ , respectively. **B**= L-isoleucyl-L-proline  $[\text{M} + \text{H}]^+$  with  $m/z$ 228), started the formation of a fragment ion at  $m/z$ 210 by the loss of  $\text{H}_2\text{O}$ , which further dissociated to produce a fragment ion at  $m/z$ 86 due to the loss of the  $(\text{C}_6\text{H}_8\text{NO}_3)$

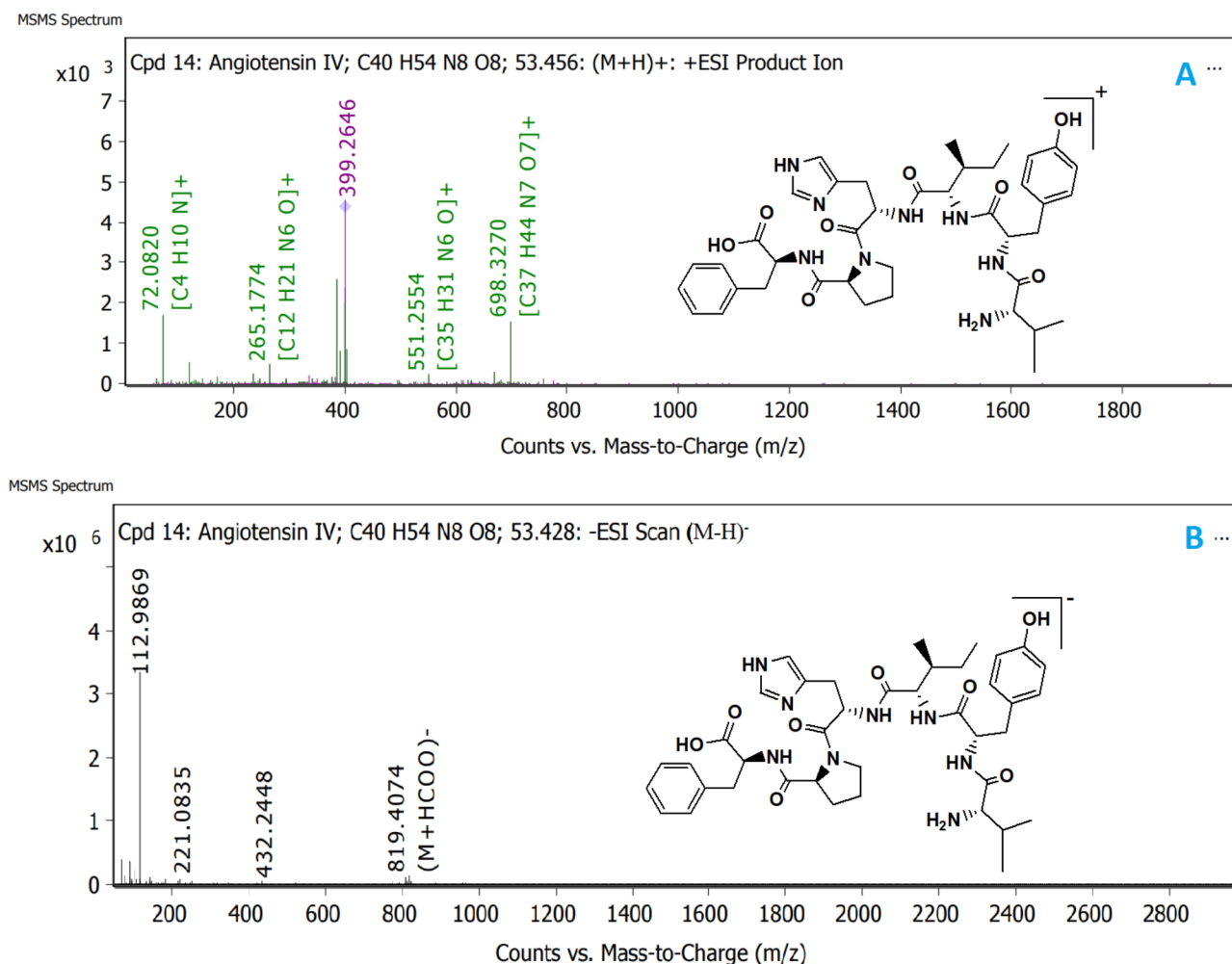


**Fig. 9** Proposed fragmentation pathways of main fragment ions for **Angiotensin IV** on the basis Q-TOF LC-MS/MS spectra in positive ionization mode  $[M+H]^+$  ions (A) and negative ionization mode  $[M-H]^-$  ions (B). See details produced **five** characteristic fragment ions at  $m/z$  698.3222, at  $m/z$  551.2648, at  $m/z$  399.2646 at  $m/z$  265.1774 and at  $m/z$  72.0826 for (A). Moreover, **three** characteristic fragment ions at  $m/z$  432.2448, at  $m/z$  221.0835 and at  $m/z$  112.9869 were formed for (B)

more informative and intense peaks than deprotonated Angiotensin IV molecules (Fig. 9A and B, Table 2A, 2B).

Bioactive peptides have been shown to have anti-inflammatory effect in macrophages by inhibiting the NO/iNOS and PGE2/COX-2 pathways while suppressing the production of pro-inflammatory cytokines such IL-1 $\beta$  and TNF- $\alpha$  [30]. When THP-1 cells were stimulated with TNF- $\alpha$ , Cysteine and Histidine reduced NF- $\kappa$ B activity [31]. It was confirmed that the polypeptide “Angiotensin IV” repressed inflammation in the brains of rats with chronic cerebral hypoperfusion (CCH), as it significantly reduced the levels of TNF- $\alpha$ , IL-1 $\beta$ , IL-6 and IL-12 in the brains of rats with CCH (CCH) [32].

#### Fatty acids

The use of Q-TOF-MS/MS allowed the identification of potential bioactive polyunsaturated fatty acids ; (2E,4E)-2,7-Dimethyl-2,4-octadienedioic acid, at  $m/z$  198.0896

$[M+H]^+$  ( $C_{10}H_{14}O_4$ ) (Rt 44.577 min), DB Diff. (-1.93); Methyl-18,18-dibromo-9E,17-octadecadien-5,7-dienoate, at  $m/z$  442.0157  $[M+H]^+$  ( $C_{19}H_{24}Br_2O_2$ ) (Rt 88.605 min) DB Diff. (-3.22); 8,12-Octadecadienoic acid at  $m/z$  280.2422  $[M+H]^+$  ( $C_{18}H_{32}O_2$ ) (Rt 89.069 min) DB Diff. (-6.97), in addition to Valproic acid at  $m/z$  144.1161  $[M+H]^+$  ( $C_8H_{16}O_2$ ) (Rt 94.533 min) DB Diff. (-1.75) (Table 2A).

In-vitro, saturated fatty acids (SFAs) were found to directly stimulate inflammatory gene expression via TLR4 signaling. The relative potency of various (SFAs) varied with chain length, with lauric acid (12:0) having the highest activity, whereas myristic acid (14:0) and stearic acid (18:0) having surprisingly little pro-inflammatory activity. Unlike SFAs, monounsaturated- fatty acids (MUFAs) and polyunsaturated fatty acids (PUFAs) did not activate TLR4 signaling. These researchers were able to demonstrate that pretreatment of cells for 3 h with a

**Table 2** Characterization of secondary metabolites from "A. Unguis isolate SP51-EGY" fungal extract by Q-TOF LC-HRMS analysis (A = positive, B = negative ionization mode)

Proposed Compounds [A]	RT (min)	Molecular Formula	Molecular Weight (m/z)	Fragment ions	Mass Error (ppm)	Ionization ESI (+)	Reference
<b>Peptides</b>							
1 Isoleucyl-Alanine	23.528	C <sub>9</sub> H <sub>18</sub> N <sub>2</sub> O <sub>3</sub>	202.1323	185.1284, 156.9625, 86.0971	-0.57	[M-H <sub>2</sub> O+H] <sup>+</sup>	[48]
2 L-isoleucyl-L-proline	27.265	C <sub>11</sub> H <sub>20</sub> N <sub>2</sub> O <sub>3</sub>	228.1483	211.1450, 183.0928	-0.9	[M-H <sub>2</sub> O+H] <sup>+</sup>	HMDB0011174
3 L-phenylalanyl-L-proline	31.723	C <sub>14</sub> H <sub>18</sub> N <sub>2</sub> O <sub>3</sub>	262.1327	245.1293, 217.1071	-0.92	[M-H <sub>2</sub> O+H] <sup>+</sup>	HMDB0011177
4 L-prolyl-L-phenylalanine	33.901	C <sub>14</sub> H <sub>18</sub> N <sub>2</sub> O <sub>3</sub>	262.1329	245.1295, 217.1013, 70.0663, 60.0840	-1.12	[M-H <sub>2</sub> O+H] <sup>+</sup>	HMDB0011179
5 <b>Angiotensin IV</b> [H-Val-Tyr-Ile-His-Pro-Phe-OH]	53.456	C <sub>40</sub> H <sub>54</sub> N <sub>8</sub> O <sub>8</sub>	774.4077	775.4149, 676.3474, 497.2835, 399.2646, 265.1774, 236.1617, 72.0820	-1.58	[M+H] <sup>+</sup>	[48]
6 Histidinyl-Cysteine	100.8	C <sub>9</sub> H <sub>14</sub> N <sub>4</sub> O <sub>3</sub> S	258.0784	241.0754, 223.0647	0.99	[M-H <sub>2</sub> O+H] <sup>+</sup>	[48]
7 Cysteinyl-Histidine	101.92	C <sub>9</sub> H <sub>14</sub> N <sub>4</sub> O <sub>3</sub> S	258.0785	241.0754, 223.0647	0.47	[M-H <sub>2</sub> O+H] <sup>+</sup>	HMDB0028777 [48]
<b>Fatty acids</b>							
8 (2E,4E)-2,7-Dimethyl-2,4-octadiene-dioic acid	44.577	C <sub>10</sub> H <sub>14</sub> O <sub>4</sub>	198.0896	181.0863, 156.1209, 129.0530, 115.9653, 95.9737,	-1.93,	[M-H <sub>2</sub> O+H] <sup>+</sup>	[48]
9 Methyl 18,18-dibromo-9E,17-octadecadien-5,7-dienoate	88.605	C <sub>19</sub> H <sub>24</sub> Br <sub>2</sub> O <sub>2</sub>	442.0157	443.0238, 425.2169, 352.3414,	-3.22	[M+H] <sup>+</sup>	(CFM-ID)
10 8,12-octadecadienoic acid	89.069	C <sub>18</sub> H <sub>32</sub> O <sub>2</sub>	280.2422	280.2654, 263.2383, 95.0864	-6.97	[M-H <sub>2</sub> O+NH <sub>4</sub> ] <sup>+</sup>	[49]
11 Butyl butyrate	93.044	C <sub>8</sub> H <sub>16</sub> O <sub>2</sub>	144.1161	145.1229, 127.1128	-7.1	[M-H <sub>2</sub> O+H] <sup>+</sup>	[48]
12 Valproic acid	94.929	C <sub>8</sub> H <sub>16</sub> O <sub>2</sub>	144.1161	127.1129,	-1.1	[M-H <sub>2</sub> O+H] <sup>+</sup>	[50]
<b>Amides</b>							
13 Palmitic amide	92.832	C <sub>16</sub> H <sub>33</sub> NO	255.2579	256.2615, 124.0879	-6.11	[M+H] <sup>+</sup>	[48]
14 Oleamide	94.533	C <sub>18</sub> H <sub>35</sub> NO	281.2736	282.2808, 127.1128	-1.75	[M+H] <sup>+</sup>	[49]
15 N-oleoyl alanine	95.485	C <sub>21</sub> H <sub>39</sub> NO <sub>3</sub>	353.2946	352.3416, 336.2913, 282.2807, 127.1128	-4.53	[M-H <sub>2</sub> O+H] <sup>+</sup>	[49]
16 Sphingosine	95.547	C <sub>18</sub> H <sub>37</sub> NO <sub>2</sub>	299.2837	282.2807, 124.0879	-4.34	[M-H <sub>2</sub> O+H] <sup>+</sup>	MassBank of Japan ( <a href="https://www.mssj.jp/">https://www.mssj.jp/</a> ), HMDB0000252 (CFM-ID)
17 D-erythro-Sphingosine C-20	100.6	C <sub>20</sub> H <sub>41</sub> NO <sub>2</sub>	327.3154	352.3413, 310.3121, 309.3143, 284.2964,	-5.16	[M-H <sub>2</sub> O+H] <sup>+</sup>	(CFM-ID)
18 Stearamide	100.9	C <sub>18</sub> H <sub>37</sub> NO	283.2891	284.2965, 223.0648, 124.0877, 116.1076	-5.73	[M+H] <sup>+</sup>	[48]

**Table 2** (continued)

Proposed Compounds [A]	RT (min)	Molecular Formula	Molecular Weight (m/z)	Fragment ions	Mass Error (ppm)	Ionization ESI (+)	Reference
19 Anandamide (20:l, n-9)	101.57	C <sub>22</sub> H <sub>43</sub> NO <sub>2</sub>	353.3311	336.3268, 317.3032, 223.0646,100.0765	-4.87	[M-H <sub>2</sub> O+H] <sup>+</sup>	HMDB0031678 [48]
20 Stearoylethanolamide	101.61	C <sub>20</sub> H <sub>41</sub> N O <sub>2</sub>	327.315	310.3121, 284.2964, 124.0878	-3.85	[M-H <sub>2</sub> O+H] <sup>+</sup>	[48]
<b>Triglycerides</b>							
21 MG(16:0/0:0/0:0)	95.338	C <sub>19</sub> H <sub>38</sub> O <sub>4</sub>	330.2785	353.2683, 331.2892, 313.2755	-4.49	[2 M+Na] <sup>+</sup>	HMDB0011533 (CFM-ID)
22 2-(14,15-Epoxyeicosat-rienoyl) Glycerol	102.5	C <sub>23</sub> H <sub>38</sub> O <sub>5</sub>	394.2735	352.3412, 285.0956, 223.0674	-3.87	[M-H <sub>2</sub> O+H] <sup>+</sup>	[48]
23 Triricinolein (triglyceride)	137.45	C <sub>57</sub> H <sub>104</sub> O <sub>9</sub>	932.7694	951.7786, 933.7768, 657.5075, 519.1396, 321.2411, 285.0956	-1.44	[M+NH <sub>4</sub> ] <sup>+</sup>	[48]
<b>Others</b>							
24 Lyciumoside IV [acyclic diterpene glycoside]	55.225	C <sub>38</sub> H <sub>64</sub> O <sub>16</sub>	776.4243	759.4209, 380.2147, 315.1830	-6.29	[M-H <sub>2</sub> O+H] <sup>+</sup>	HMDB0033499 [48]
25 Hydroxy ibuprofen	62.635	C <sub>13</sub> H <sub>18</sub> O <sub>3</sub>	222.1267	227.1053, 205.1232, 187.1127, 157.0480	-4.8	[M-H <sub>2</sub> O+Na] <sup>+</sup>	[48]
26 trans-Resveratrol	68.579	C <sub>14</sub> H <sub>12</sub> O <sub>3</sub>	228.0797	233.0583, 211.0765, 197.9894, 185.0427	-4.63	[M-H <sub>2</sub> O+Na] <sup>+</sup>	[48]
27 Eszopiclone	80.271	C <sub>17</sub> H <sub>17</sub> Cl N <sub>6</sub> O <sub>3</sub>	388.1059	411.0957, 389.1132, 371.1047, 352.3411, 129.0533	-2.27	[M+Na] <sup>+</sup>	[48]
28 Zopiclone	82.176	C <sub>17</sub> H <sub>17</sub> Cl N <sub>6</sub> O <sub>3</sub>	388.1058	411.0954, 389.1133, 371.1094, 352.3410, 129.0532	-1.8	[M+Na] <sup>+</sup>	[48]
29 Methenolone	89.075	C <sub>20</sub> H <sub>30</sub> O <sub>2</sub>	302.2237	302.2472, 167.0564	0.87	[M-H <sub>2</sub> O+NH <sub>4</sub> ] <sup>+</sup>	HMDB0041928 [48]
30 2,4,6-Triethyl-1,3,5-trithiane	101.92	C <sub>9</sub> H <sub>18</sub> S <sub>3</sub>	222.0574	223.0647, 124.0877	-0.36	[M+H] <sup>+</sup>	[48]
31 Rifamycin O	125.81	C <sub>39</sub> H <sub>47</sub> N O <sub>14</sub>	753.2991	772.2763, 667.1737, 519.1405, 223.0647	0.78	[M-H <sub>2</sub> O+K] <sup>+</sup>	(CFM-ID)
32 Uroporphyrin I	139.85	C <sub>40</sub> H <sub>38</sub> N <sub>4</sub> O <sub>16</sub>	830.2347	848.2731, 832.2411, 758,2226	-7.73	[M+NH <sub>4</sub> ] <sup>+</sup>	[48]
33 Vitisifuran A	150.31	C <sub>56</sub> H <sub>40</sub> O <sub>12</sub>	904.252	124.0877	0.02	[M+NH <sub>4</sub> ] <sup>+</sup>	HMDB0034785 [48]

**Table 2** (continued)

Proposed Compounds [A]	RT (min)	Molecular Formula	Molecular Weight (m/z)	Fragment ions	Mass Error (ppm)	Ionization ESI (+)	Reference
<b>Proposed Compounds [B]</b>	<b>RT (min)</b>	<b>Molecular Formula</b>	<b>Molecular Weight (m/z)</b>	<b>Fragment ions</b>	<b>Mass Error (ppm)</b>	<b>Ionization ESI (-)</b>	<b>Reference</b>
<b>Peptides</b>							
1	5-Methoxy-DL-tryptophan	C <sub>12</sub> H <sub>14</sub> N <sub>2</sub> O <sub>3</sub>	234.1019	215.0841, 112.9868	-6.04	[M-H <sub>2</sub> O-H] <sup>-</sup>	[48]
2	Angiotensin IV	C <sub>40</sub> H <sub>54</sub> N <sub>8</sub> O <sub>8</sub>	774.4093	433.256, 221.129, 114.056	-3.67	[M+HCOO] <sup>-</sup>	Manually confirmed
3	Se- Adenosylseleno-homo- cysteine	C <sub>14</sub> H <sub>20</sub> N <sub>6</sub> O <sub>5</sub> Se	426.0666	407.0482, 248.9631	5.41	[M-H <sub>2</sub> O-H] <sup>-</sup>	HMDB0011117 [48]
<b>Fatty acids</b>							
4	Isopropyl 3-(3,4-dihydroxy phenyl)-2-hydroxypropanoate	C <sub>12</sub> H <sub>16</sub> O <sub>5</sub>	240.1013	221.0835, 112.9868	-6.51	[M-H <sub>2</sub> O-H] <sup>-</sup>	[48]
5	3-carboxy-4-methyl-5-propyl-2-furan-propanoic acid	C <sub>12</sub> H <sub>16</sub> O <sub>5</sub>	240.1014	238.9334, 221.0836	-6.86	[M-H <sub>2</sub> O-H] <sup>-</sup>	HMDB0061112 [48]
6	(2E,4E)-2,7-Dimethyl-2,4-octadiene-dioic acid	C <sub>10</sub> H <sub>14</sub> O <sub>4</sub>	198.0907	198.0907, 179.0728	-7.66	[M-H <sub>2</sub> O-H] <sup>-</sup>	HMDB0034099 [48]
7	18,18-dibromo-9E,17-octadecadien-5,7-diyonic acid	C <sub>18</sub> H <sub>24</sub> Br <sub>2</sub> O <sub>2</sub>	428	426.9936, 248.9628	-3.18	[M-H] <sup>-</sup>	(CFM-ID)
8	9R,10 S-dihydroxy-stearic acid	C <sub>18</sub> H <sub>36</sub> O <sub>4</sub>	316.2636	316.2636, 112.9869	-2.2	[M+CH <sub>3</sub> COO] <sup>-</sup>	HMDB0302281 [49]
<b>Triglyceride</b>							
9	MG(0:0/18:0/0:0) [monoglyceride]	C <sub>21</sub> H <sub>42</sub> O <sub>4</sub>	358.3105	403.3084, 358.3105	-5.98	[M+HCOO] <sup>-</sup>	[48] HMDB0011535
10	Triricinolein (triglyceride)	C <sub>57</sub> H <sub>104</sub> O <sub>9</sub>	932.772	,297.2455,	-4.24	[M+HCOO] <sup>-</sup>	HMDB0038061 [48]
<b>Halogenated, phenolic compounds and glycosides</b>							
11	5-Hydroxythalidomide	C <sub>13</sub> H <sub>10</sub> N <sub>2</sub> O <sub>5</sub>	274.0607	255.0447,	-1.71	[M-H <sub>2</sub> O-H] <sup>-</sup>	HMDB0013871 [48]
12	Granisetron	C <sub>18</sub> H <sub>24</sub> N <sub>4</sub> O	312.1955	293.1776	-1.69	[M-H <sub>2</sub> O-H] <sup>-</sup>	[48]
13	Sulfasalazine	C <sub>18</sub> H <sub>14</sub> N <sub>4</sub> O <sub>5</sub> S	398.0692	398.0692, 371.1158	-0.71	[M+HCOO-H <sub>2</sub> O] <sup>-</sup>	HMDB0014933 [49]
14	Fenofibric acid	C <sub>17</sub> H <sub>15</sub> ClO <sub>4</sub>	318.0679	359.0714,	-6.4	[M+CH <sub>3</sub> COO-H <sub>2</sub> O] <sup>-</sup>	HMDB0252207 MassBank of Japan ( <a href="https://www.mssj.jp/">https://www.mssj.jp/</a> ) [48]
15	Umbelliprenin [coumarin]	C <sub>24</sub> H <sub>30</sub> O <sub>3</sub>	366.2186	383.1782, 347.2017, 248.9632, 112.9868	2.49	[M+Cl-H <sub>2</sub> O] <sup>-</sup>	[48]
16	Alpha-CEHC (alpha-Carboxyethylhydroxy-chroman)	C <sub>16</sub> H <sub>22</sub> O <sub>4</sub>	278.1537	277.1464, 248.6929	-6.31	[M-H] <sup>-</sup>	[48]
17	4-Dodecylbenzenesulfonic acid	C <sub>18</sub> H <sub>30</sub> O <sub>3</sub> S	326.1936	325.1863, 293.1811,	-6.24	[M-H] <sup>-</sup>	[49]
18	Naficillin	C <sub>21</sub> H <sub>22</sub> N <sub>2</sub> O <sub>5</sub> S	414.1253	459.1240, 415.0301, 325.1864,	-0.36	[M+HCOO] <sup>-</sup>	[48]
19	Persicachrome	C <sub>25</sub> H <sub>36</sub> O <sub>3</sub>	384.2641	384.2641, 365.2487	2.31	[M-H <sub>2</sub> O-H] <sup>-</sup>	HMDB0036425 [48]
20	Lyciumoside IV, [acyclic diterpene glycoside]	C <sub>38</sub> H <sub>64</sub> O <sub>16</sub>	776.4251	803.4128, 776.4251	-7.3	[M+HCOO-H <sub>2</sub> O] <sup>-</sup>	HMDB0033499 [49]
21	Piceid (Resveratrol glycoside)	C <sub>20</sub> H <sub>22</sub> O <sub>8</sub>	390.1336	390.1336, 371.1158	-5.53	[M-H <sub>2</sub> O-H] <sup>-</sup>	HMDB0031422 [48]

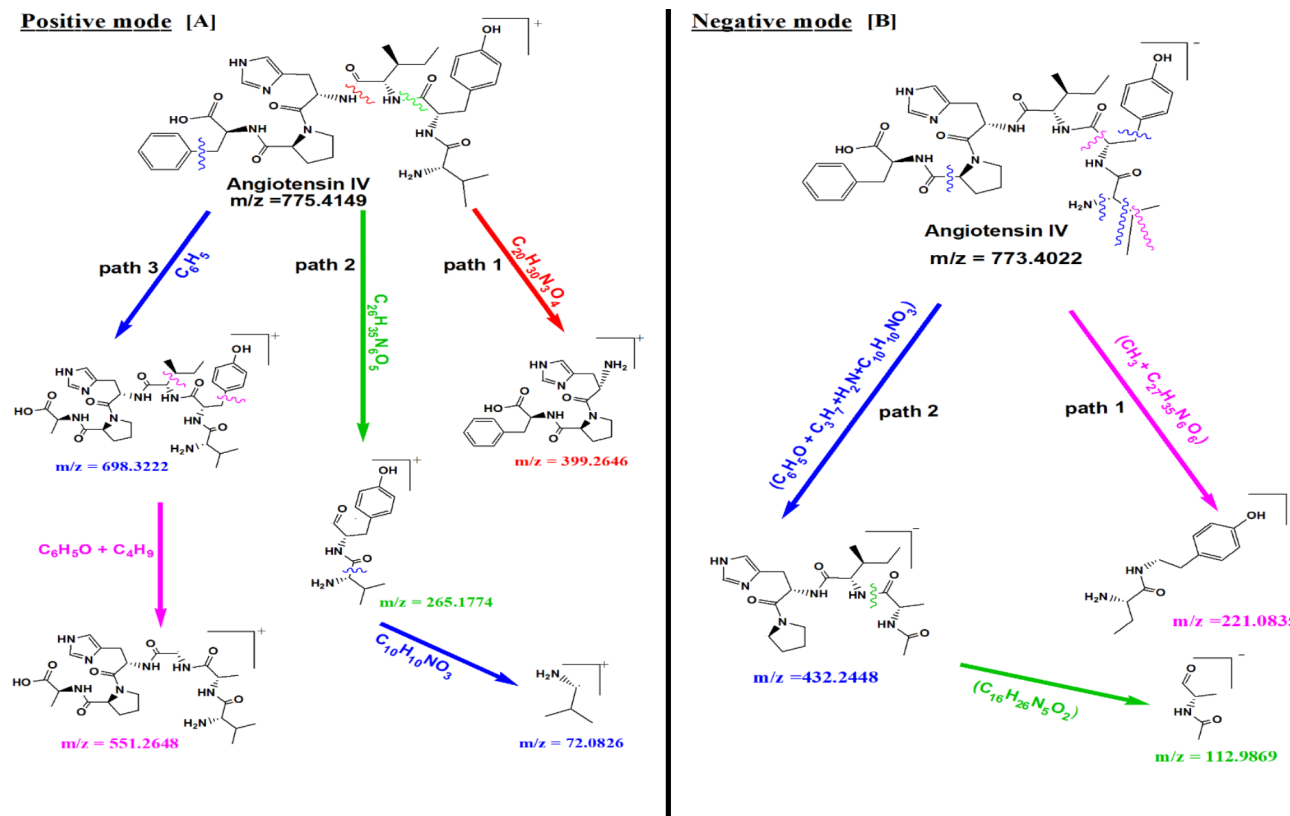


**Fig. 10** Comparison of the fragmentation pattern of the MS/MS spectrum demonstrated that (A) Protonated Angiotensin IV molecule give more informative and more intense peaks than do (B) deprotonated Angiotensin IV molecule

variety of PUFAs or oleic acid (18:1) significantly reduced the subsequent pro-inflammatory effect of lauric acid treatment. They went on to demonstrate that PUFAs' ability to inhibit inflammatory responses induced by LPS or lauric acid was dependent on TLR4 [33]. Valproic acid (VPA) inhibits the CD45<sup>high</sup>F4/80<sup>low</sup> macrophage subset as well as the production of pro-inflammatory cytokines/chemokines such as CXCL1, IL-5, IL-6, and IL-10. (VPA) specifically decreased tissue NF- $\kappa$ B p100 protein [34].

#### Amides

In Q-TOF LC-HRMS positive ionization mode analysis, eight amides were identified (Table 2A).

Anti-inflammatory activity has previously been reported for oleamide and anandamide (20:l, n-9).

The identified constituents were found at  $m/z$  281.2736  $[M+H]^+$  ( $C_{18}H_{35}NO$ ) (Rt 94.533 min) DB Diff. (-1.75) and at  $m/z$  353.3311  $[M+H]^+$  ( $C_{22}H_{43}NO_2$ ) (Rt 101.57 min) DB Diff. (-1.72), respectively.

**Fatty acid amides**, played critical roles in inflammation suppression [35]. Oleamide suppressed LPS-induced iNOS and COX-2 mRNA in RAW 264.7 cells, as well as inflammatory cytokines; TNF- $\alpha$ , IL-1 $\beta$  and IL-6 [36]. Anandamide inhibited NO and IL-6 release by LPS-stimulated J774 macrophages, as well as IL-12 and IL-23

production and increased IL-10 production by activated microglia via JNK and ERK1/2 activation and NF- $\kappa$ B [37].

#### Other compounds

In addition; ten other compounds were identified, three of which were previously reported to have anti-inflammatory effect; **Hydroxy-ibuprofen**, at  $m/z$  222.1267  $[M+H]^+$  ( $C_{13}H_{18}O_3$ ) (Rt 62.635 min) DB Diff. (-1.07), **Resveratrol** at  $m/z$  228.0797  $[M+H]^+$  ( $C_{14}H_{12}O_3$ ) (Rt 68.579 min) DB Diff. (-1.06) and **Rifamycin-O** at  $m/z$  753.2991  $[M+H]^+$  ( $C_{39}H_{47}NO_{14}$ ) (Rt 125.81 min) DB Diff. (0.59) (Table 2A).

**Hydroxy Ibuprofen** is an Ibuprofen metabolite. Ibuprofen is an anti-inflammatory agent with IC50s of 13 M and 370 M for COX-1 and COX-2, respectively [38]. **Resveratrol** was a potent inhibitor of the NO and cytokine release in activated macrophages and microglia [39]. **Rifamycin-O** also antagonized TNF- $\alpha$  and LPS-induced NF- $\kappa$ B activities and inhibited IL1 $\beta$ -induced synthesis of inflammatory chemokine, IL8 [40].

#### Q-TOF LC-HRMS analysis [negative ionization mode]

Furthermore, negative ionization mode was mainly characterized by the identification of fatty acids, phenolic and glycoside compounds (Table 2B).

### Peptides

Two peptides were only identified in negative ionization mode: Angiotensin IV and Se-Adenosylseleno-homocysteine. In addition, the amino acid; **5-methoxy-DL-Tryptophan** with Rt (33.421 min), M Wt. ( $m/z$  234.1019,  $C_{12}H_{14}N_2O_3$ ), DB Diff. (-6.04) was identified (Table 2B). 5-methoxy-DL-Tryptophan reduces LPS-induced expression of COX-2, TNF- $\alpha$ , IL-1 $\beta$ , and IL-6 in RAW 264.7 macrophages [41].

### Fatty acids

Five fatty acids were identified, one of which was Iso-propyl-3-(3,4-dihydroxyphenyl)-2-hydroxypropanoate (**IDHP**); with Rt (43.097 min), M Wt. ( $m/z$  240.1013,  $C_{12}H_{16}O_5$ ), DB Diff. (-6.51) (Table 2B). (**IDHP**) drastically reduced NO, TNF- $\alpha$ , and IL-1 $\beta$  production in LPS-induced BV-2 cells and rat primary microglia. IDHP also suppressed LPS-induced iNOS, TNF- $\alpha$ , and IL-1 $\beta$  mRNA expression [42].

### Halogenated, phenolic compounds and glycosides

Furthermore, eleven compounds were identified in negative ionization mode, from which the followings : **Granisetron**, Rt (63.003 min), M Wt. ( $m/z$  312.1955,  $C_{18}H_{24}N_4O$ ), DB Diff. (-1.69), **Fenofibric acid**, Rt (68.719 min), M Wt. ( $m/z$  318.0679,  $C_{17}H_{15}ClO_4$ ), DB Diff. (-6.4), **Umbelliprenin**, Rt (72.239 min), M Wt. ( $m/z$  366.2186,  $C_{24}H_{30}O_3$ ), DB Diff. (2.49), **Alpha-CEHC**, Rt (74.282 min), M Wt. ( $m/z$  278.1537,  $C_{16}H_{22}O_4$ ), DB Diff. (-6.31) and **Piceid**, Rt (66.684 min), M Wt. ( $m/z$  390.1336,  $C_{20}H_{22}O_8$ ), DB Diff. (-5.53) (Table 2B), were previously reported to have anti-inflammatory activity.

The amide "**Granisetron**" significantly reduced TNF- $\alpha$ , IL-6, HMGB1, and NF- $\kappa$ B. It also reduced the expression of the receptor for advanced glycation end, TLR4, in liver tissue, as well as pyroptosis, by decreasing NLRP3, IL-1 $\beta$ , and caspase-1 [43]. **Fenofibrate** decreases the expression and secretion of TNF- $\alpha$ , IL-1 $\beta$ , and IL-6 via the NF- $\kappa$ B signaling pathway, making them therapeutic targets for attenuating inflammation in hepatic pathological progression [44].

**Umbelliprenin** (UMB), a natural sesquiterpene coumarin, may reduce inflammation by lowering IL-17 levels in the blood. **UMB** exerts its anti-inflammatory effects by modulating distinct cytokine release/inhibition types [45]. **Alpha-CEHC** is a vitamin E derivative that reduces LPS-induced gene expression of TNF- $\alpha$ , IL-1 $\beta$ , IL-6, and iNOS. While high concentrations increased gene expression in peritoneal macrophages [46]. Studies in rat models have indicated that vitamin E exhibits anti-inflammatory properties by suppressing IL-1 and IL-6. Vitamin E has also been shown to inhibit COX-2, the enzyme involved in inflammatory reactions [47]. **Piceid** is a Resveratrol glycoside: Resveratrol inhibited NO and

cytokine release in activated macrophages and microglia [39].

### Conclusions

The intricate interplay of TLR4 in immune responses underscores its dual role as both protector and potential provocateur. Malfunctioning TLR4 signaling can inadvertently amplify immune responses, thereby inducing conditions like sepsis, acute lung injury, and pathological chronic inflammation, often linked to cancer and autoimmune maladies. Central to this inflammatory response is the production of NO by iNOS, which triggers the subsequent activation TNF- $\alpha$ , and IL-6. Notably, this study delved into the potential Nrf2-dependency of the anti-inflammatory properties of "*Aspergillus unguis* isolate SP51-EGY" extracts, revealing their effects to be independent of Nrf2 modulation. A significant modulation in the expression of inflammatory markers, such as iNOS, COX-2, TNF- $\alpha$ , and IL-6 was observed using real-time qPCR. The extract labeled (B Sh F) was particularly potent in this regard. Further chemical profiling of this extract via Q-TOF LC-HRMS unveiled a rich tapestry of 54 bioactive compounds, with several playing pivotal roles in inflammation suppression. Key compounds such as granisetron, fenofibrate, and umbelliprenin were shown to attenuate inflammatory pathways, particularly the NF- $\kappa$ B signaling cascade. Marine-associated fungi, like the "*Aspergillus unguis* isolate SP51-EGY" from the Red Sea, have emerged as bounteous reservoirs of secondary metabolites, displaying diverse biological activities and intricate structures. This study not only underscores the potential of LC-HRMS as a formidable analytical tool but also highlights the pressing need for further research into the bioaccessibility, bioavailability, and toxicological profiles of these fungal extracts. Future endeavors should also encompass animal model studies, paving the way for the potential therapeutic commercialization of these promising extracts.

### Abbreviations

COX-2	Cyclooxygenase-2
ELISA	Enzyme-linked immunosorbent assay
HO-1	Heme oxygenase 1
iNOS	Inducible nitric oxide synthase
IL-1	Interleukin-1
IL-6	Interleukin-6
LPS	Lipopolysaccharide
LC-HRMS	Liquid chromatography-high-resolution mass spectrometry
NO	Nitric oxide
Nrf2	Nuclear factor erythroid 2-related factor 2
NF- $\kappa$ B	Nuclear factor-kappa B
OSGIN1	Oxidative stress induced growth inhibitor 1
PUFAs	Polyunsaturated fatty acids
qPCR	Quantitative real-time polymerase chain reaction
TLRs	Toll-Like Receptors
TNF- $\alpha$	Tumor necrosis factor alpha
UMB	Umbelliprenin

## Supplementary Information

The online version contains supplementary material available at <https://doi.org/10.1186/s12896-024-00890-1>.

Supplementary Material 1

### Acknowledgements

Not applicable.

### Author contributions

S.N., A.S.D., A.M.I., M.S.A., W.F., A.A., and F.K.A.E. contributed to the study conception and design. Material preparation, data collection, and analysis were performed by S.N. and A.S.D. LC/MS/MS part is interpreted, discussed, and written by F.K.A.E. and A.M.I. S.N., and A.S.D. wrote the first draft of the manuscript, and all authors commented on previous versions. S.N., A.S.D., A.M.I., M.S.A., W.F., A.A., and F.K.A.E. read and approved the final manuscript.

### Funding

This work was financially supported by a Bartlett Fund for Critical Challenges, an ASRT grant to A.A., and the bilateral projects within the Executive Program of Scientific and Technological Cooperation between the Arab Republic of Egypt and the Italian Republic under Project No. [A2-12-15] to F.K.A.E. Open access funding provided by The Science, Technology & Innovation Funding Authority (STDF) in cooperation with The Egyptian Knowledge Bank (EKB).

### Data availability

The raw data supporting the conclusions of this article will be made available by the authors, without unjustified reservation.

### Declarations

#### Ethics approval and consent to participate

Not applicable.

#### Consent for publication

Not applicable.

#### Competing interests

The authors declare no competing interests.

#### Author details

<sup>1</sup>Institute of Global Health and Human Ecology, School of Sciences and Engineering, The American University in Cairo (AUC), P.O. Box: 74, Cairo 11835, Egypt

<sup>2</sup>Biochemical Engineering Department, Faculty of Energy and Environmental Engineering, The British University in Egypt, Suez Desert Road, P.O. Box: 43, El-Shorouk City, Cairo 11837, Egypt

<sup>3</sup>Chemistry of Natural and Microbial Products Department, National Research Centre, Giza 12622, Egypt

<sup>4</sup>Department of Microbial Chemistry, National Research Centre, Giza 12622, Egypt

<sup>5</sup>Drug Bioassay-Cell Culture Laboratory, Pharmacognosy Department, National Research Centre, Giza 12622, Egypt

Received: 6 October 2023 / Accepted: 28 August 2024

Published online: 18 September 2024

## References

- Chen L, Deng H, Cui H, Fang J, Zuo Z, Deng J, et al. Inflammatory responses and inflammation-associated diseases in organs. *Oncotarget*. 2017;9(6):7204–18. <https://doi.org/10.18632/oncotarget.23208>.
- Saleh HA, Yousef MH, Abdelnaser A. The anti-inflammatory properties of Phytochemicals and their effects on epigenetic mechanisms involved in TLR4/NF- $\kappa$ B-Mediated inflammation. *Front Immunol*. 2021;12. <https://doi.org/10.3389/fimmu.2021.606069>. <https://www.frontiersin.org/articles/>.
- Newton K, Dixit VM. Signaling in Innate immunity and inflammation. *Cold Spring Harb Perspect Biol*. 2012;4(3):a006049. <https://doi.org/10.1101/cshperspect.a006049>.
- Mohan S, Gupta D. Crosstalk of toll-like receptors signaling and Nrf2 pathway for regulation of inflammation. *Biomed Pharmacother*. 2018;108:1866–78. <https://doi.org/10.1016/j.biopha.2018.10.019>.
- Sukkar MB, Harris J. Potential impact of oxidative stress induced growth inhibitor 1 (OSGIN1) on airway epithelial cell autophagy in chronic obstructive pulmonary disease (COPD). *J Thorac Disease*. 2017;9(12):4825–7. <https://doi.org/10.21037/jtd.2017.10.153>.
- Schink A, Neumann J, Leifke AL, Ziegler K, Fröhlich-Nowoisky J, Cremer C, et al. Screening of herbal extracts for TLR2- and TLR4-dependent anti-inflammatory effects. *PLoS ONE*. 2018;13(10):e0203907. <https://doi.org/10.1371/journal.pone.0203907>.
- Tasneem S, Liu B, Li B, Choudhary MI, Wang W. Molecular pharmacology of inflammation: Medicinal plants as anti-inflammatory agents. *Pharmacol Res*. 2019;139:126–40. <https://doi.org/10.1016/j.phrs.2018.11.001>.
- Wu B, Wiese J, Labes A, Kramer A, Schmaljohann R, Imhoff JF. Lindgomycin, an unusual antibiotic polyketide from a Marine Fungus of the Lindgomycetaceae. *Mar Drugs*. 2015;13(8):4617–32. <https://doi.org/10.3390/md13084617>.
- Youssef FS, Ashour ML, Singab ANB, Wink M. A comprehensive review of bioactive peptides from Marine Fungi and their biological significance. *Mar Drugs*. 2019;17(10):559. <https://doi.org/10.3390/md17100559>.
- Razzaghi-Abyaneh M, Rai M, Razzaghi-Abyaneh M, Rai M. The genus aspergillus - pathogenicity, mycotoxin production and industrial applications. 2022. <https://doi.org/10.5772/intechopen.94793>. [Accessed 3rd February 2023].
- Aboutabl ME, Maklad YA, Abdel-Aziz MS, El-Hady FKA. In vitro and in vivo studies of the antidiabetic potential of Red Sea sponge-associated fungus aspergillus unguis isolate SP51-EGY with correlations to its chemical composition. *J Appl Pharm Sci*. 2022;12(8):165–78. <https://doi.org/10.7324/JAPS.2022.120817>.
- Aydoğan C. Recent advances and applications in LC-HRMS for food and plant natural products: a critical review. *Anal Bioanal Chem*. 2020;412(9):1973–91. <https://doi.org/10.1007/s00216-019-02328-6>.
- Dawood AS, Sedeeq MS, Farag MA, Abdelnaser A. Terfezia boudieri and terfezia claveryi inhibit the LPS/IFN- $\gamma$ -mediated inflammation in RAW 264.7 macrophages through an Nrf2-independent mechanism. *Sci Rep*. 2023;13(1):10106. <https://doi.org/10.1038/s41598-023-35612-8>.
- Wynn TA, Chawla A, Pollard JW. Macrophage biology in development, homeostasis and disease. *Nature*. 2013;496(7446):445–55. <https://doi.org/10.1038/nature12034>.
- Watanabe S, Alexander M, Misharin AV, Budinger GRS. The role of macrophages in the resolution of inflammation. *J Clin Investig*. 129(7): 2619–28. <https://doi.org/10.1172/JCI124615>.
- Kwon DH, Cha HJ, Choi EO, Leem SH, Kim GY, Moon SK, et al. Schisandrin A suppresses lipopolysaccharide-induced inflammation and oxidative stress in RAW 264.7 macrophages by suppressing the NF- $\kappa$ B, MAPKs and PI3K/Akt pathways and activating Nrf2/HO-1 signaling. *Int J Mol Med*. 2018;41(1):264–74. <https://doi.org/10.3892/ijmm.2017.3209>.
- Joo T, Sowndhararajan K, Hong S, Lee J, Park SY, Kim S, et al. Inhibition of nitric oxide production in LPS-stimulated RAW 264.7 cells by stem bark of Ulmus pumila L. *Saudi J Biol Sci*. 2014;21(5):427–35. <https://doi.org/10.1016/j.sjbs.2014.04.003>.
- Xu J, Yi M, Ding L, He S. A review of anti-inflammatory compounds from Marine Fungi, 2000–2018. *Mar Drugs*. 2019;17(11):636. <https://doi.org/10.3390/md17110636>.
- Nguyen TQC, Duy Binh T, Pham TLA, Nguyen YDH, Thi Xuan Trang D, Nguyen TT, et al. Anti-inflammatory effects of Lasia spinosa Leaf Extract in Lipopolysaccharide-Induced RAW 264.7 macrophages. *Int J Mol Sci*. 2020;21(10):3439. <https://doi.org/10.3390/ijms21103439>.
- Elsayed EA, El Enshasy H, Wadaan MAM, Aziz R, Mushrooms. A potential natural source of anti-inflammatory compounds for medical applications. *Mediat Inflamm*. 2014;2014:e805841. <https://doi.org/10.1155/2014/805841>.
- Anh CV, Yoon YD, Kang JS, Lee HS, Heo CS, Shin HJ. Nitrogen-Containing secondary metabolites from a deep-sea fungus aspergillus unguis and their anti-inflammatory activity. *Mar Drugs*. 2022;20(3):217. <https://doi.org/10.3390/md20030217>.
- Cao VA, Kwon JH, Kang JS, Lee HS, Heo CS, Shin HJ. Aspersterols A–D, ergostane-type sterols with an unusual Unsaturated Side Chain from the Deep-Sea-Derived Fungus Aspergillus Unguis. *J Nat Prod*. 2022;85(9):2177–83. <https://doi.org/10.1021/acs.jnatprod.2c00398>.

23. Brennan MS, Matos MF, Richter KE, Li B, Scannevin RH. The NRF2 transcriptional target, OSGIN1, contributes to monomethyl fumarate-mediated cytoprotection in human astrocytes. *Sci Rep*. 2017;7(1):42054. <https://doi.org/10.1038/srep42054>.
24. Chen XL, Dodd G, Thomas S, Zhang X, Wasserman MA, Rovin BH, et al. Activation of Nrf2/ARE pathway protects endothelial cells from oxidant injury and inhibits inflammatory gene expression. *Am J Physiol Heart Circ Physiol*. 2006;290(5):H1862–70. <https://doi.org/10.1152/ajpheart.00651.2005>.
25. Saha S, Buttari B, Panieri E, Profumo E, Saso L. An overview of Nrf2 Signaling Pathway and its role in inflammation. *Molecules*. 2020;25(22):5474. <https://doi.org/10.3390/molecules25225474>.
26. Abdulkhaleq LA, Assi MA, Abdullah R, Zamri-Saad M, Taufiq-Yap YH, Hezme MNM. The crucial roles of inflammatory mediators in inflammation: a review. *Veterinary World*. 2018;11(5):627–35. <https://doi.org/10.14202/vetworld.2018.627-635>.
27. Turner MD, Nedjai B, Hurst T, Pennington DJ. Cytokines and chemokines: at the crossroads of cell signalling and inflammatory disease. *Biochim et Biophys Acta (BBA) - Mol Cell Res*. 2014;1843(11):2563–82. <https://doi.org/10.1016/j.bbamcr.2014.05.014>.
28. Germolec DR, Shipkowski KA, Frawley RP, Evans E. Markers of inflammation. In: DeWitt JC, Rockwell CE, Bowman CC, editors. *Immunotoxicity testing: methods and protocols*. New York, NY: Springer; 2018. pp. 57–79. [https://doi.org/10.1007/978-1-4939-8549-4\\_5](https://doi.org/10.1007/978-1-4939-8549-4_5). [Accessed 25th December 2021].
29. Ghanim AM, Girgis AS, Kariuki BM, Samir N, Said MF, Abdelnaser A, et al. Design and synthesis of ibuprofen-quinoline conjugates as potential anti-inflammatory and analgesic drug candidates. *Bioorg Chem*. 2022;119:105557. <https://doi.org/10.1016/j.bioorg.2021.105557>.
30. Lee SH, Lee H, Kim JC. Anti-inflammatory effect of water extracts obtained from *doenjang* in LPS-stimulated RAW 264.7 cells. *Food Sci Technol*. 2019;39:947–54. <https://doi.org/10.1590/ft.15918>.
31. Hasegawa S, Ichiyama T, Sonaka I, Ohsaki A, Hirano R, Haneda Y, et al. Amino acids exhibit anti-inflammatory effects in human monocytic leukemia cell line, THP-1 cells. *Inflamm Res*. 2011;60(11):1013–9. <https://doi.org/10.1007/s00011-011-0362-1>.
32. Wang QG, Xue X, Yang Y, Gong PY, Jiang T, Zhang YD. Angiotensin IV suppresses inflammation in the brains of rats with chronic cerebral hypoperfusion. *J Renin-Angiotensin-Aldosterone Syst*. 2018;19(3):1470320318799587. <https://doi.org/10.1177/1470320318799587>.
33. Fritsche KL. The science of fatty acids and inflammation. *Adv Nutr*. 2015;6(3). <https://doi.org/10.3945/an.114.006940>. 293S–301S.
34. Seet LF, Toh LZ, Finger SN, Chu SWL, Wong TT. Valproic acid exerts specific cellular and molecular anti-inflammatory effects in post-operative conjunctiva. *J Mol Med*. 2019;97(1):63–75. <https://doi.org/10.1007/s00109-018-1722-x>.
35. Barata PHS, Sarquis IR, Carvalho HO, Barros AS, Rodrigues AB, Galue-Parra AJ, et al. Chemoenzymatic synthesis and anti-inflammatory activity of fatty acid Amides prepared from *Bertholletia excelsa* (Brazil Nut) triglycerides. *J Braz Chem Soc*. 2020;31:1557–65. <https://doi.org/10.21577/0103-5053.20200041>.
36. Moon SM, Lee SAH, Hong JH, Kim JS, Kim DK, Kim CS. Oleamide suppresses inflammatory responses in LPS-induced RAW264.7 murine macrophages and alleviates paw edema in a carrageenan-induced inflammatory rat model. *Int Immunopharmacol*. 2018;56:179–85. <https://doi.org/10.1016/j.intimp.2018.01.032>.
37. Rahaman O, Ganguly D. Endocannabinoids in immune regulation and immunopathologies. *Immunology*. 2021;164(2):242–52. <https://doi.org/10.1111/imm.13378>.
38. He Y, Langenhoff AAM, Sutton NB, Rijnaarts HHM, Blokland MH, Chen F, et al. Metabolism of Ibuprofen by *Phragmites australis*: Uptake and Phytodegradation. *Environ Sci Technol*. 2017;51(8):4576–84. <https://doi.org/10.1021/acs.est.7b00458>.
39. Steiner N, Balez R, Karunaweera N, Lind JM, Münch G, Ooi L. Neuroprotection of Neuro2a cells and the cytokine suppressive and anti-inflammatory mode of action of resveratrol in activated RAW264.7 macrophages and C8–B4 microglia. *Neurochem Int*. 2016;95:46–54. <https://doi.org/10.1016/j.neuint.2015.10.013>.
40. Rosette C, Agan FJ, Rosette N, Moro L, Mazzetti A, Hassan C, et al. Rifamycin SV exhibits strong anti-inflammatory in vitro activity through pregnane X receptor stimulation and NFκB inhibition. *Drug Metab Pharmacokinet*. 2019;34(3):172–80. <https://doi.org/10.1016/j.dmpk.2019.01.002>.
41. Wang YF, Hsu YJ, Wu HF, Lee GL, Yang YS, Wu JY, et al. Endothelium-derived 5-Methoxytryptophan is a circulating anti-inflammatory molecule that blocks systemic inflammation. *Circul Res*. 2016;119(2):222–36. <https://doi.org/10.1161/CIRCRESAHA.116.308559>.
42. Wang S, Wang H, Jing H, Wang S, Kang L, Gao X, et al. Anti-inflammatory effects of isopropyl 3-(3, 4-dihydroxyphenyl)-2-hydroxypropanoate, a novel metabolite from danshen, on activated microglia. *Chin J Physiol*. 2012;55(6):428–34. <https://doi.org/10.4077/cjp.2011.amm045>.
43. Aboyoussif AM, Mohammad MK, Abo-Saif AA, Messiha BAS. Granisetron attenuates liver injury and inflammation in a rat model of cecal ligation and puncture-induced sepsis. *J Pharmacol Sci*. 2021;147(4):358–66. <https://doi.org/10.1016/j.jphs.2021.08.005>.
44. Won TW. Fenofibrate, a peroxisome proliferator-activated receptor α-agonist, blocks lipopolysaccharide-induced inflammatory pathways in mouse liver. *Korean J Hepato-Biliary-Pancreatic Surg*. 2013;17(3):89. <https://doi.org/10.14701/kjhbps.2013.17.3.89>.
45. Shirani K, Iranshahi M, Askari VR, Gholizadeh Z, Zadeh AA, Zeinali M, et al. Comparative evaluation of the protective effects of oral administration of auraptene and umbelliprenin against CFA-induced chronic inflammation with polyarthritis in rats. *Biomed Pharmacother*. 2021;139:111635. <https://doi.org/10.1016/j.biopha.2021.111635>.
46. Qureshi AA, Reis JC, Papisian CJ, Morrison DC, Qureshi N. Tocotrienols inhibit lipopolysaccharide-induced pro-inflammatory cytokines in macrophages of female mice. *Lipids Health Dis*. 2010;9(1):143. <https://doi.org/10.1186/1476-511X-9-143>.
47. Dar KB, Khan IS, Amin S, Ganie AH, Bhat AH, Dar SA, et al. Active Cousinia thomsonii extracts modulate expression of crucial Proinflammatory Mediators/Cytokines and NFκB Cascade in Lipopolysaccharide-Induced albino Wistar Rat Model. *J Inflamm Res*. 2020;13:829–45. <https://doi.org/10.2147/JIR.S272539>.
48. Allen F, Greiner R, Wishart D. Competitive fragmentation modeling of ESI-MS/MS spectra for putative metabolite identification. *Metabolomics*. 2015;11(1):98–110. <https://doi.org/10.1007/s11306-014-0676-4>.
49. Wang F, Liigand J, Tian S, Arndt D, Greiner R, Wishart DS. CFM-ID 4.0: more accurate ESI-MS/MS spectral prediction and compound identification. *Anal Chem*. 2021;93(34):11692–700. <https://doi.org/10.1021/acs.analchem.1c01465>.
50. Wishart DS, Knox C, Guo AC, Eisner R, Young N, Gautam B, et al. HMDB: a knowledgebase for the human metabolome. *Nucleic Acids Res*. 2009;37(Database issue):D603–10. <https://doi.org/10.1093/nar/gkn810>.

## Publisher's note

Springer Nature remains neutral with regard to jurisdictional claims in published maps and institutional affiliations.